

93

01

08

15

THE FORMATION AND EARLY EVOLUTION OF STARS
AN OBSERVATIONAL PERSPECTIVE

CHARLES J. LADA
Smithsonian Astrophysical Observatory
60 Garden Street
Cambridge, Massachusetts, 02138, USA

ABSTRACT

To understand the origin of stars is one of the most challenging and important quests of modern astrophysical research. During the twentieth century, observational and theoretical evidence has clearly established that star formation is occurring in the present epoch of galactic history. Yet, the process of star formation itself has never been directly observed, having long been shrouded in mystery by veils of obscuring interstellar dust. During the last 25 years advances in observational technology have begun to penetrate these dusty obscuring shrouds to reveal an increasingly clear picture of the physical processes involved in the formation and early evolution of stars. As a result the foundations for the development of a physical theory of star formation are being laid. In these lectures I will attempt to document the observational underpinnings of the present state of knowledge concerning the star formation process in our Galaxy.

1. The Continuing Process of Star Formation

The question of the origin of stars is one of the most fundamental of astronomy. Yet, despite thousands of years of stellar observation, and early speculations by Newton and Laplace, it has only been in the latter part of the present century that the investigation of star formation has become an active discipline of astrophysical research. That the origin of stars has remained so mysterious for so long is largely due to the fact that the process of star formation has never been directly observed either with the naked eye or the with most powerful telescopes. Moreover, prior to the twentieth century neither the energy source nor the bulk composition of stars were known. Indeed, without knowledge of the physical nature of stars it was very difficult to develop an understanding of their origin. At the end of the nineteenth century, the nature of the mystery surrounding stellar origins was nicely summed up by the fictional character Huck Finn (in the book *The Adventures of Huck Finn* by Mark Twain) when he observed the stars in the night sky and wondered "...*did they just happen or was they made?*"

Have the stars been around since creation or were they being made in the heavens? As far as anybody could tell at dawn of this century, the entire universe consisted of a single stellar system, stars lived forever and the question of the origin of stars was a question of cosmology. As such the problem of star formation was not susceptible to detailed scientific investigation. That is, even the most basic hypotheses concerning

stellar origins could not be directly tested by observation. Fortunately, over the last half century astronomical research has led to the fundamental realization that star formation has been a continuous, ongoing process throughout the history of the Galaxy and the universe. This critical fact has been demonstrated by both theory and observation.

Perhaps the most important step contributing to this realization was the discovery of the nature of stars as natural thermonuclear reactors which fuse hydrogen, the primary product of the Big Bang, into helium and then ultimately into the heavier elements which make up the periodic table. This process is elegantly explained by the theory of stellar structure and evolution, perhaps the greatest theoretical achievement of twentieth century astronomy. Although this great theory does not in any way account for or predict the formation of stars (and is in this sense incomplete), it has successfully explained the basic physical properties of stars as well as the processes of stellar evolution and death once stars exhaust their nuclear fuel reserves. In particular, stellar evolution theory demonstrated that certain luminous stars, OB stars, burn their nuclear fuel at such prodigious rates that they can live for only a small fraction of the lifetime of our galaxy. The existence of such stars clearly indicates that star formation is occurring in the present epoch of Galactic history.

The relative youth of OB stars was also clearly demonstrated by observations of their spatial distribution on the sky. In 1947 the Armenian astronomer V.A. Ambartsumian showed that OB stars were almost always members of stellar groupings he termed OB Associations. Furthermore he found that the space densities of stars in OB associations were well below the threshold necessary to prevent their disruption by Galactic tidal forces. Ambartsumian calculated dynamical ages for the associations that were much less than the age of the galaxy. These dynamical ages turned out to be in good agreement with the nuclear ages of the stars and independently provided evidence that star formation is still an active process in the Galaxy.

The discovery of the interstellar medium of gas and dust during the early part of the twentieth century provided a crucial piece of corroborating evidence in support of the concept of present epoch Galactic star formation. Subsequent observations of interstellar material established that clouds of interstellar gas and dust had roughly stellar composition and were considerably more massive than a single star or group of stars. This revealed that the raw material to make new stars was relatively abundant in the Galaxy. These three pieces of evidence, 1) stellar evolution theory, 2) expanding OB associations and 3) the interstellar medium, constitute three basic "proofs" of ongoing star formation in the Milky Way.

Because star formation is occurring in the present epoch, the question of the origin of stars can be investigated by direct observation. If this were not the case, the prospects for completing the theory of stellar structure and evolution with a description of how stars form would be bleak. Yet, for most of the century, direct observation of the star formation process and the development of a theory to explain it, were severely hampered by the fact that most stars form in dark clouds and during their formative stages are invisible optically. Fortunately, advances in observational technology over the last quarter century opened the infrared and millimeter-wave

windows to astronomical investigation and enabled direct observations of star forming regions and this has significantly expanded our knowledge of the star formation process. As a result the foundations for a coherent theory of star formation and early evolution are being laid. The observational underpinnings of such a theory are the subject of the rest of these lectures.

2. Stellar Observations: The Fossil Record

2.1. Clustering and Multiplicity

Stars in the disk of our galaxy can be categorized by their spatial distribution as being either members of the general Galactic field population or members of associations or clusters. An association or cluster is defined as a group of stars of the same physical type whose surface density significantly exceeds that of the field for stars of the same physical type³. Associations differ from clusters in their space densities: associations have space densities well below that (i.e., $0.1 M_{\odot} \text{pc}^{-1}$)⁴ required for stability against galactic tides while clusters have space densities (e.g., $\geq 1.0 M_{\odot} \text{pc}^{-1}$) considerably in excess of the tidal stability limit. The spatial extents of associations are typically very large, 50- 150 parsecs, while clusters are typically small in size (≈ 1 parsec in diameter). Only a very small fraction of the stars in the disk of the Galaxy are presently members of associations or clusters. However, virtually all known O stars are members of OB associations. This indicates that all O stars formed in OB associations and results from the fact that the dynamical ages of OB associations (i.e., approximately 10^7 years) are greater than the lifetimes of the individual O stars ($\sim 10^6$ yrs.). About 10% of all B stars are members of associations. But when one takes into account that the lifetime of a B star is an order of magnitude larger than the lifetime of an association, it is clear that all present day B stars probably formed in OB associations.^{1,5}

OB associations contain considerably more low mass stars than OB stars, but the spatial density of these fainter stars is not that much greater than that of faint field stars. Consequently, the low mass component of OB associations is very difficult to identify from stellar density counts alone. If a stellar association is sufficiently young ($\leq 2 - 3 \times 10^6$ yrs.) then many of its low mass stars are likely to be emission-line (T Tauri type) stars. Emission-line stars are relatively rare in the field and groups of young, low mass T-Tauri stars can be easily identified as T associations. In most instances T associations spatially coexist with OB associations⁷ and trace the low mass component of such stellar groups. As will be discussed later, observations of very young associations (those embedded in molecular clouds) suggest the ratio of OB stars to low mass stars is roughly given by the initial mass function for local field stars. Consequently, it follows that OB associations can account for the formation of nearly all stars being born in the present epoch of galactic history. However, it is interesting to note that if OB associations were producing stars over the age of the Galaxy at the rate currently observed they would account for only about 10% of the stellar mass of the Milky Way. Open clusters are stellar systems which are stable against galactic tides and have considerably longer lifetimes (10^8 yrs.) than

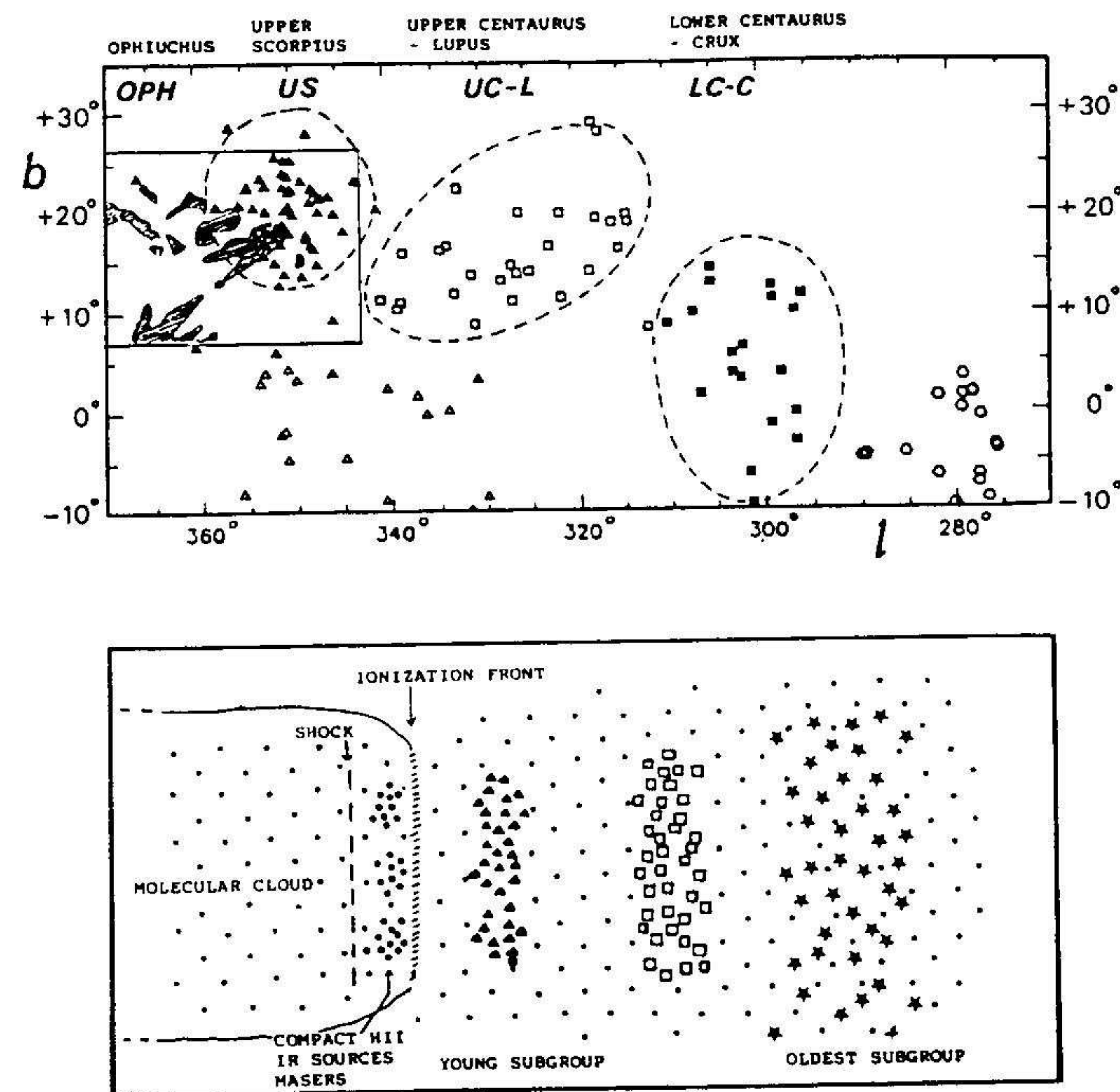


Figure 1: (Top) Positions of OB stars in the Oph-Sco-Cen Association. The subgroups are outlined and a sketch of the dark clouds in the Ophiuchus region is also shown. (Bottom) A schematic diagram illustrating the Elmegreen-Lada sequentially triggered star formation model for OB subgroups. Figure adapted from Blaauw⁵.

associations. Roughly 10% of all stars being formed end up as members of bound open clusters.¹ However most open clusters themselves probably formed inside OB associations.

The internal radial velocity dispersions of OB association members are typically on the order of $2-3 \text{ km s}^{-1}$. It is important to bear in mind that even in the absence of galactic tidal forces, these motions are too large to allow the associations to be bound by self-gravity. It has long been recognized that OB associations could provide important information about the star formation process since they are so young that the individual members have not had enough time to move very far from their places of birth. For example, the present sizes of OB associations must closely reflect the sizes of the clouds which spawned them.^{5,6,7} In addition, the structure of OB associations can provide important fossil clues about the structure and even the temporal evolution of a star forming complex. One common property of OB associations is that they are sub-structured, often consisting of sub-groupings of sequentially differing age.² Such

sub-structure has suggested that star formation proceeds through a star forming region in an ordered temporal sequence. The chain reaction like nature of the spatial-temporal structure of OB subgroups has led to the suggestion that OB subgroups are formed by a process of sequential triggering.⁷

The tendency for stars to form in groups is not limited to associations and clusters. On much smaller, more intimate size scales (i.e., 1-100 AU) we find that most stars are members of binary or multiple star systems. For example, radial velocity measurements of field G dwarf stars indicate that roughly 57% of all such stars have stellar companions.^{8,9} The binarity fraction does not appear to depend too strongly on spectral type as studies of both M dwarfs⁴⁵ and B stars¹¹ have indicated. Since some binaries may have been disrupted since formation, these fractions could be lower limits to the actual fraction of binary stars produced in the star formation process. Binary stars provide a strong constraint for star formation theories. In this regard, it is interesting to note that the mass of binary companions seems to be independent of the mass of their primaries.⁹

2.2. The Initial Mass Function

A fundamental consequence of the theory of stellar evolution is that the life history of a star is almost entirely pre-determined by its initial mass. Consequently, to understand star formation and the consequent luminosity evolution of the galaxy requires a detailed knowledge of both the initial distribution of stellar masses at birth and how this quantity varies through space and time within the galaxy. Unfortunately, stellar evolution theory is not able to predict the Initial Mass Function (IMF) of stars. This quantity must be derived from observations. However, to do so is not straightforward because stellar mass is not itself an observable quantity. Stellar radiant flux or luminosity is the most readily observed property of a star. Therefore, the starting point of any attempt to determine a stellar mass spectrum is the determination of a stellar luminosity function. Then, an appropriate mass-luminosity relation is required to transform the luminosity function into a stellar mass function.

The first attempt to derive an empirical initial mass spectrum was carried out by Salpeter¹³ who used as a starting point the general (or van Rhijn) luminosity function determined for field stars within the neighborhood of the sun. The field star luminosity function, $\Phi(M_V)$, is the relative number of stars per unit magnitude interval per unit volume of space as a function of absolute magnitude, M_V , in the solar neighborhood. (The determination of the field star luminosity function is itself a difficult task and discussion of this is beyond the scope of this lecture, and the reader who desires more information on this topic is referred to the text by Mihalas and Binney¹²). In principle, the field star luminosity function counts all presently visible field stars in the neighborhood of the sun. Because stars more massive than the sun have main sequence lifetimes shorter than that of the galaxy they are under represented in the field star luminosity function with respect to low mass stars, whose lifetimes are in excess of the age of the galaxy. Therefore, the present day field star luminosity function is biased toward low luminosity stars and must be corrected for the effects of post-main-sequence stellar evolution to obtain a luminosity function

more representative of that produced at stellar birth.

Salpeter introduced the concept of an initial luminosity function, $\Psi(M_V)$, which is the relative number of stars per unit volume in each absolute magnitude interval originally produced by the star formation process. He derived $\Psi(M_V)$ from the field star luminosity function as follows:

$$\Psi(M_V) = \Phi(M_V) \quad \text{for} \quad \tau_{MS} \geq \tau_{MW}$$

and

$$\Psi(M_V) = \frac{\tau_{MW}}{\tau_{MS}} \Phi(M_V) \quad \text{for} \quad \tau_{MS} < \tau_{MW}$$

where τ_{MW} is the age of the galaxy and τ_{MS} is the main sequence lifetime of a star under consideration. Here, it has been assumed for simplicity that the stellar birthrate and the form of $\Psi(M_V)$ has been constant with time over the age of the galaxy. To derive an initial distribution of stellar mass we need to apply a mass luminosity relation to $\Psi(M_V)$. With the additional assumption that $\Psi(M_V)$ counts only main sequence stars, we can use the empirical mass-luminosity relation for main sequence stars (i.e., $L_* \sim m_*^p$, where $p \approx 3.45$).^{14,15} Because $\Psi(M_V)$ is a distribution of stellar (absolute, visual) magnitudes and not luminosities, it is convenient to use a form of the mass-luminosity relation that relates M_V to stellar mass. Since $L_* \sim m_*^p$, and $M_V \sim \log L_*$, then $M_V \sim \log m_*$. Consequently it is useful to introduce the concept of the initial mass function $\xi(\log m_*)$ which is the relative number of stars formed per unit volume per unit *logarithmic* mass interval and is straightforwardly related to $\Psi(M_V)$ as follows:

$$\Psi(M_V)dM_V = \xi(\log m_*)d\log m_*$$

The shape of the initial mass function is usually characterized by a spectral index, $\beta \equiv \partial \log \xi(\log m_*) / \partial \log m_*$, which is the slope of the function in a log-log plot. We note that the initial mass spectrum, $f(m_*)$, (i.e., the differential frequency distribution of stellar masses at birth) is related to the mass function by:

$$\xi(\log m_*) = \frac{m_* f(m_*)}{0.434}$$

The spectral index of the mass spectrum, γ , is equal to $\beta - 1$.

Salpeter found that the initial mass function (IMF) could be reasonably well represented by a simple power-law form viz:

$$\xi(\log m_*) \sim m_*^{-1.35}$$

In other words, a constant spectral index over the range of stellar mass that was considered, between approximately 0.4 and 10 M_\odot . In addition, the value of the spectral index (being less than -1.0) indicated that more stellar mass was contained in low mass stars than in high mass stars.

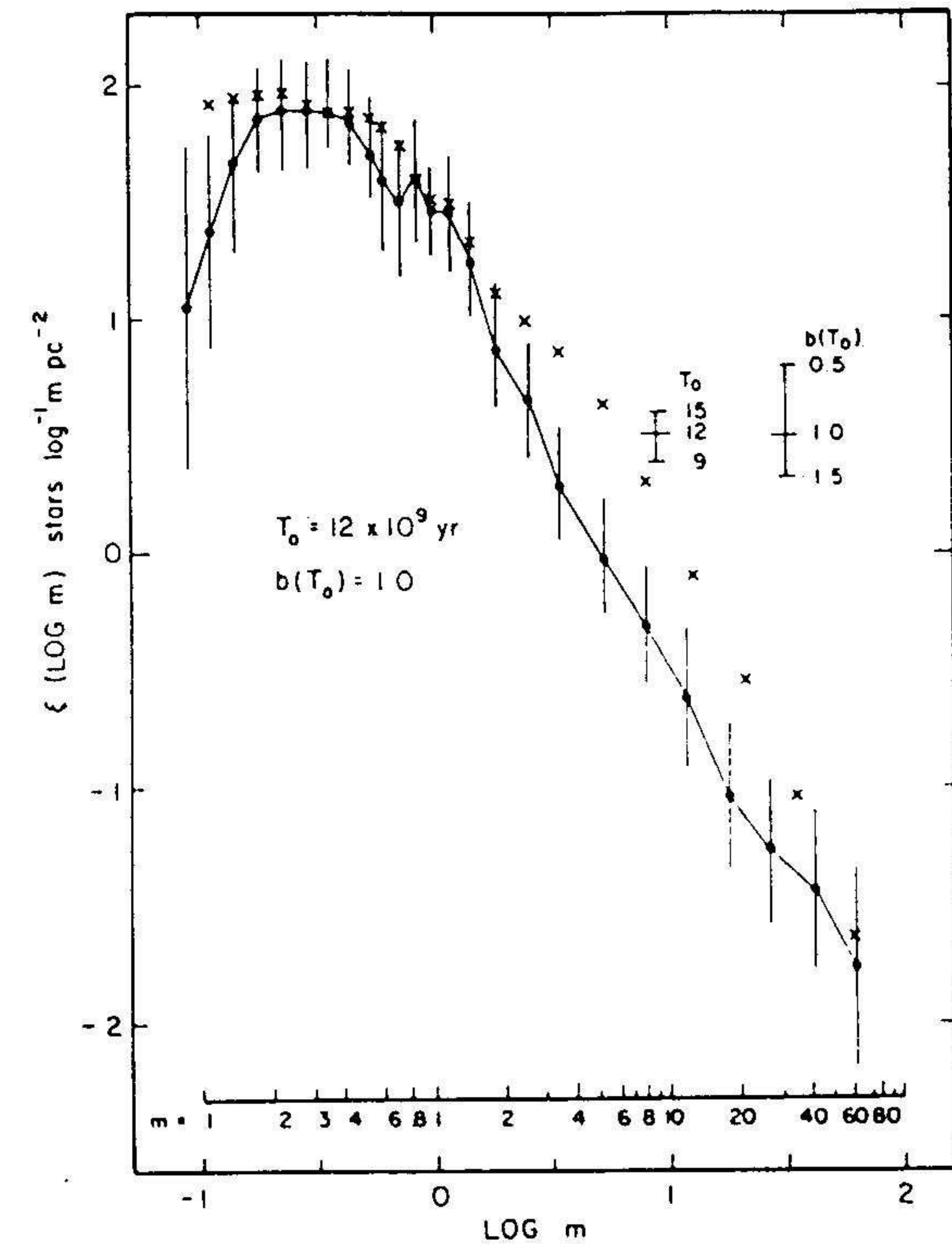


Figure 2: The IMF for field stars derived by Scalo¹⁶. Uncertainties are indicated along with bars which show the effects of varying the assumptions of birthrate $b(T_0)$ and disk age T_0 .

However, more recent and detailed studies¹⁶ suggest that the field star IMF is not characterized by a single spectral index. Figure 2 shows the IMF derived by Scalo.¹⁶ The Scalo IMF has two notable qualities. First at intermediate and high stellar masses, it has roughly a power-law shape as it rises with decreasing stellar mass. At relatively low masses ($0.5 M_\odot$) it departs strongly from a power law form and flattens with decreasing mass. There is also some evidence that the IMF turns over for masses less than about $0.3 M_\odot$. Although whether it remains flat or has a peak at roughly $0.3 M_\odot$ is the subject of some debate.¹⁷ In any event it is clear that most stars that form in the galaxy are low mass objects and that there may be a characteristic mass for star formation of around $0.3 M_\odot$.

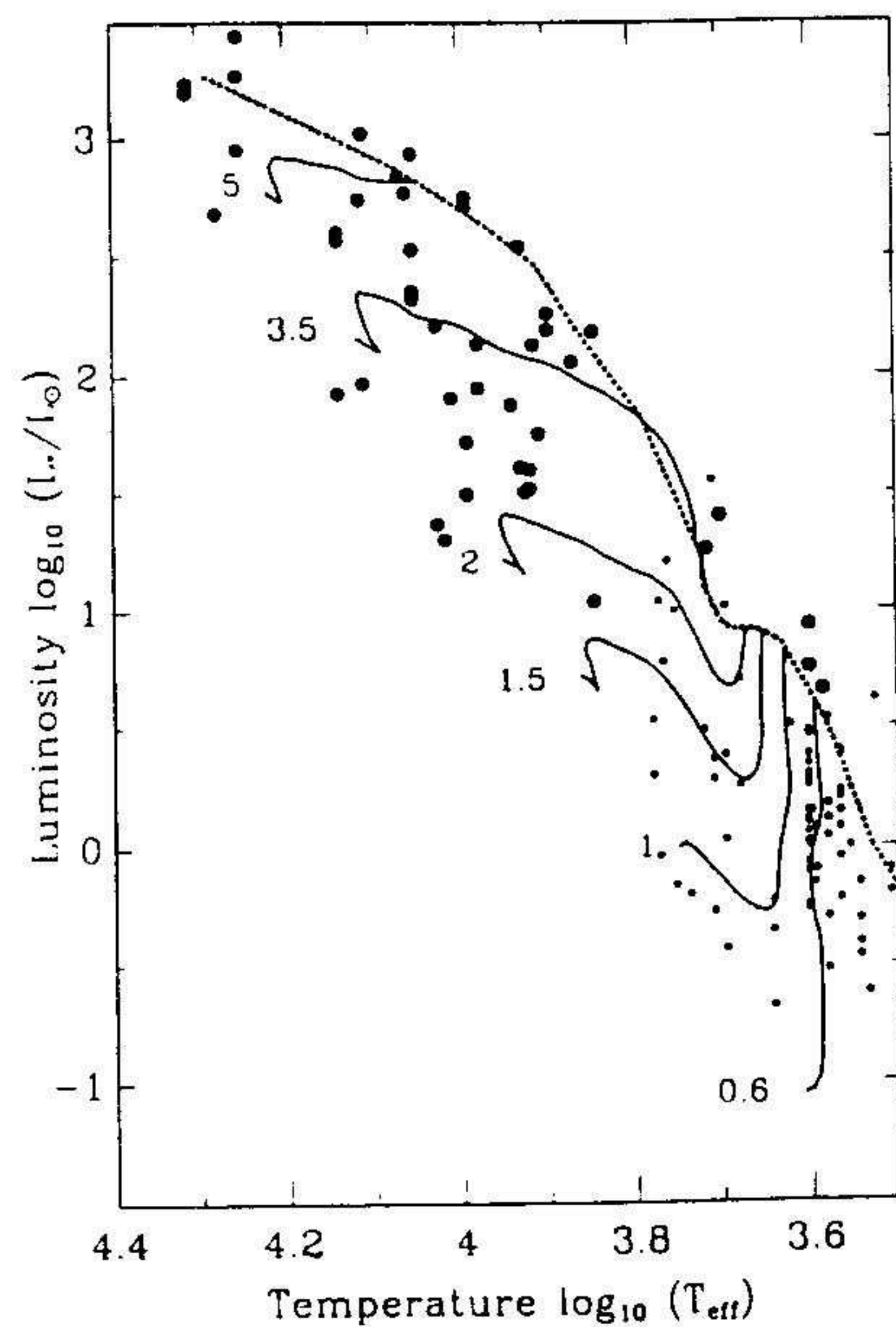


Figure 3: The HR diagram for a selection of pre-main sequence stars taken from a paper by Palla and Stahler¹⁹. Theoretical tracks (solid curves) for selected stellar masses are shown along with the birthline (dotted curve).

2.3. The HR Diagram and Early Stellar Evolution

The HR diagram is a very powerful tool for studying stellar evolution. Throughout most of its life a star will appear on the main sequence (the locus of positions in the HR diagram for stable hydrogen burning stars). The location of a star on the main sequence is determined solely by its mass. The main sequence lifetime of a star is also a very strong function of its mass. The more massive a star the shorter its main sequence lifetime. The utility of the HR diagram for investigating stellar evolution is best illustrated by its application to stellar clusters. In particular, the locations of cluster stars in the HR diagram with respect to the main sequence are determined primarily by the age of the cluster. For example, nearly 40 years ago a photometric study of the young cluster NGC 2264 by Walker¹⁸ showed that most of the stars in this group, specifically all stars with spectral types later than about A0, were characterized by luminosities and effective temperatures which placed them above the main sequence in the subgiant region of the HR diagram (just below the locations one would expect to find red giants and long period variables). That the more massive stars with earlier spectral types were found to be on the main sequence strongly suggested that the population of subgiant stars in this cluster were pre-main

sequence stars rather than post-main sequence stars. That is, these stars were not yet hydrogen burning objects. Many of these pre-main sequence stars turned out to be emission-line, T-Tauri type stars. This observation thus provided strong confirming evidence in support of the notion that T associations are very young.

Stellar evolution theory predicts that pre-hydrogen burning stars will lie above the main sequence and describes in detail the early evolution of such stars in the HR diagram. Figure 3 shows the HR diagram for a selection of pre-main sequence stars with masses between roughly $0.5-5 M_{\odot}$.¹⁹ These pre-main sequence stars form a band stretching across the HR diagram parallel the main sequence which forms its lower boundary. The fact that this band has a distinct upper envelope is very significant. This upper boundary, termed the "birthline"²⁰, marks the positions of young stars when they first appear on the HR diagram. For a star of a given mass this position corresponds to a specific size or stellar radius. In other words, a star first becomes observable and appears on the HR diagram only after it obtains a specific maximum size evidently pre-determined by its prior protostellar evolution. The birthline represents the initial condition for pre-main sequence (quasi-static) contraction. It is the dividing line between the protostellar and pre-main sequence stages of stellar evolution. Stellar evolution theory does not predict the existence of the birthline. Indeed, when evolving off the main sequence a star will expand to a size well beyond its birthline position. The physics which determine the birthline are the mysterious physics of protostellar evolution. Understanding the nature of protostars is, at present, the major frontier of star formation research.

Once a star reaches the birthline its subsequent evolution in the HR diagram depends on its mass. The theoretical evolutionary trajectories or tracks of 6 stars ranging in mass from $0.6 M_{\odot}$ to $5 M_{\odot}$ are plotted in Figure 3. Low mass stars start out as fully convective stars and descend to the main sequence along nearly vertical trajectories or convective tracks.²¹ The lowest mass stars remain fully convective until they reach the main sequence. Stars with masses of about $0.8 M_{\odot}$ or greater develop radiative interiors before reaching the main sequence. That is, the conditions in the interiors of these stars make it easier for them to transport energy outward by radiation than convection. According to the theory, once a star is radiative its luminosity is primarily dependent on its mass. This holds for any radiative star whether or not it is on the main sequence or is a post- or pre-main sequence object. Thus, such radiative stars evolve to (or away from) the main sequence with roughly constant luminosity on more or less horizontal (radiative) tracks on the HR diagram.²² Stars with masses greater than about $3 M_{\odot}$ miss the (pre-main sequence) convective phase altogether. Pre-main sequence evolutionary tracks are useful not only for determining the masses of pre-main sequence stars but also for determining their ages *subsequent to their appearance on the birthline*. Prior to their appearing on the birthline, stars are in the protostellar stage of evolution and for reasons to be discussed later cannot be placed in the HR diagram. Finally we point out that only low mass stars are expected to have a pre-main sequence phase of evolution. This is illustrated by the fact that the birthline intersects the main sequence for stars of roughly $8 M_{\odot}$. Stars more massive than this begin to burn hydrogen and reach the main sequence before their

protostellar stage of evolution ends. The physical reason for this becomes apparent if one compares the timescale for pre-main sequence evolution with that of protostellar collapse. The timescale for the gravitational collapse of a cloud core, the free-fall time, is determined largely by ρ , the density of the cloud:

$$\tau_{ff} = \sqrt{\frac{3\pi}{32G\rho}}$$

For the typical mean density ($n \approx 10^4 \text{ cm}^{-3}$) of a cloud core (of either low or high mass) the free-fall time is about 4×10^5 years. The time scale for pre-hydrogen burning evolution is the Kelvin-Helmoltz time:

$$\tau_{KH} \approx \frac{GM_*^2}{R_*L_*}$$

which is very rapid for a high mass star (i.e., $\approx 10^4$ years for $M_* = 50 M_\odot$) and relatively slow for a low mass star (i.e., $\approx 3 \times 10^7$ years for $M_* = 1 M_\odot$). More importantly for high mass stars $\tau_{KH} < \tau_{ff}$ and these stars begin burning hydrogen and reach the main sequence before the termination of the infall or collapse phase of protostellar evolution. On the other hand, for low mass stars $\tau_{KH} > \tau_{ff}$ and low mass stars have an *observable* pre-main sequence stage of stellar evolution.

3. Giant Molecular Clouds: Sites Star Formation

3.1. OB Associations and GMCs

As mentioned earlier, stars in OB associations are still very near the locations where they were born. It is therefore not surprising that OB associations are invariably associated with visible manifestations of interstellar gas and dust.² In particular, virtually all known OB associations are spatially associated with Giant Molecular Clouds.^{6,7,23} A good example of this is shown in Figure 4 which plots the positions of the OB subgroups in the Ori I association along with a map of the Orion GMC. The Orion region illustrates three important properties of OB associations and their associated GMCs: 1) The dimensions of the GMC are comparable if not larger than those of the OB association. 2) The OB subgroups display a sequential progression in age with the youngest (in this case the Trapezium cluster) usually exciting an HII region (in this case the famous Orion Nebula) or reflection nebula and therefore demonstrating a *physical* relation to the GMC. 3) The mass of the GMC ($\approx 2 - 3 \times 10^5 M_\odot$) is considerably larger than that of the OB association ($\approx 10^3 M_\odot$). From these three considerations it follows that that OB associations, and consequently most all stars currently forming in the galaxy, are born in GMCs.

The large difference between the stellar mass of the OB association and the molecular cloud (3) illustrates a fundamental property of star formation in GMCs. Namely, that the star formation efficiency (SFE=stellar mass/(stellar + gaseous mass)) in GMCs is low. For example, in the λ Ori OB association a direct comparison of the

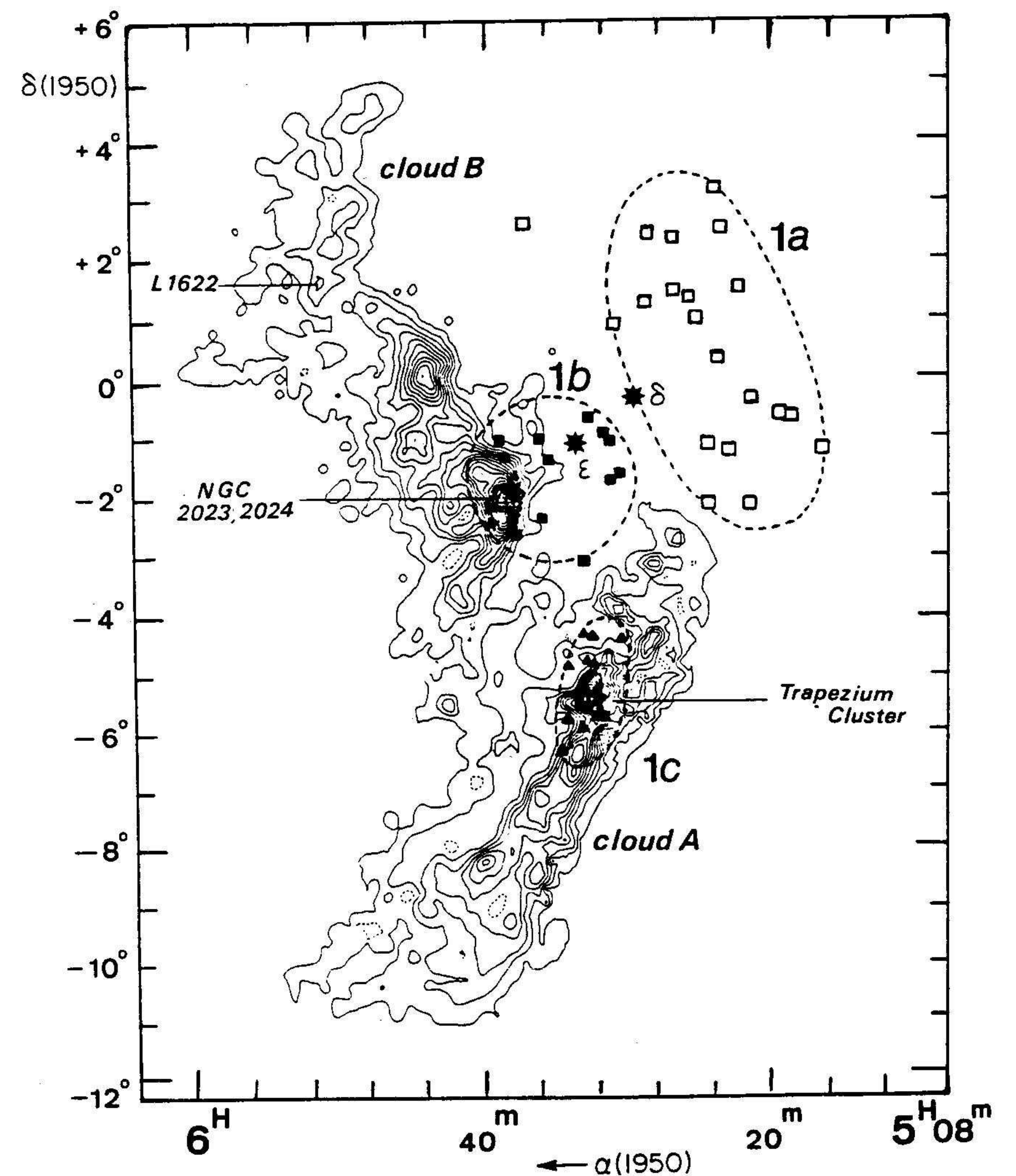


Figure 4: The ORI OB1 association and its Giant Molecular Cloud Complex. The 4 subgroups of sequentially differing age are enclosed by dashed lines. The oldest (1a) is significantly more expanded than the youngest (Trapezium Cluster). Figure taken from Blaauw⁵.

stellar and molecular mass of the star forming complex yielded an observed efficiency of only 0.3%.²⁶ Although this is probably a lower limit to the true efficiency, it likely falls short by no more than a factor of 3. Thus we expect typical SFEs of at most a few % in GMCs which when combined with the estimates of $10^9 M_{\odot}$ for the total mass of GMCs in the Galaxy and 10^7 yrs. for the typical lifetimes of GMCs, results in a star formation rate that is consistent with the overall rate for the galaxy of roughly $2-3 M_{\odot} \text{ yr}^{-1}$, derived from other observations.²⁵

The low efficiency of star formation in GMCs is of central importance for understanding the dynamical nature of OB associations. The unbound state of stellar associations is a natural consequence of star formation with a low conversion efficiency of gas to stars followed by a rapid removal of the unprocessed gas from the system.^{26,28} Figure 5 is a schematic sketch which depicts the evolution of star formation in a GMC and the creation of an expanding association.²⁸ First, low mass stars form in dense cores located throughout the cloud converting roughly 1-3% of the total gaseous mass into stars. At some point massive O stars form in the cloud and heat, ionize and disrupt the molecular gas. (We note here that it is not clear at the present time whether most of the low mass stars are formed prior to the O stars or whether the episode of O star formation is also accompanied by an increase in the production of low mass stars.) In a relatively short time ($\approx 10^6$ years), the O stars disrupt the entire complex and remove the vast majority of the original binding mass of the system. (Calculations show that O stars can disrupt an entire GMC if only 4% of the total cloud mass is converted into stars with a normal IMF.)²⁷ The stars in the cloud, which were originally orbiting in virial equilibrium with the deep potential well of the massive GMC, respond to the rapid removal of the majority of the binding mass by freely expanding into space with their initial virial velocities. This hypothesis predicts that the velocity dispersion of stars in an OB association should be on the same order of that of the molecular gas in a GMC (i.e., $2-4 \text{ km s}^{-1}$) which agrees with observations as discussed earlier.⁵ In addition it is interesting to note that the angular sizes of OB subgroups within an association increase with age of the subgroup in a manner which is consistent with typical expansion velocities (of about 2 km s^{-1})^{2,5} (see also Figure 4). The very few associations that are not near a GMC, such as Cas-Tau or Lac OB1 are associated with smaller molecular clouds and moreover have ages of ≈ 20 million years, making them among the oldest OB associations known.⁵ They have probably existed long enough to have completely disrupted their parental GMCs.

3.2. Physical Properties of GMCs

With sizes on the order of 100 pc GMCs are the largest known objects in the Galaxy. Moreover, with masses in excess of $10^5 M_{\odot}$, GMCs rival globular clusters as the most massive objects in the Milky Way. Molecular clouds are characterized by gas kinetic temperatures in the range between 10-50 K making them the coldest objects in the universe. There are a few thousand GMCs in the Galaxy and they account for a substantial fraction of all interstellar matter. Giant molecular clouds are composed primarily of hydrogen which is mostly molecular in form due to the low temperatures

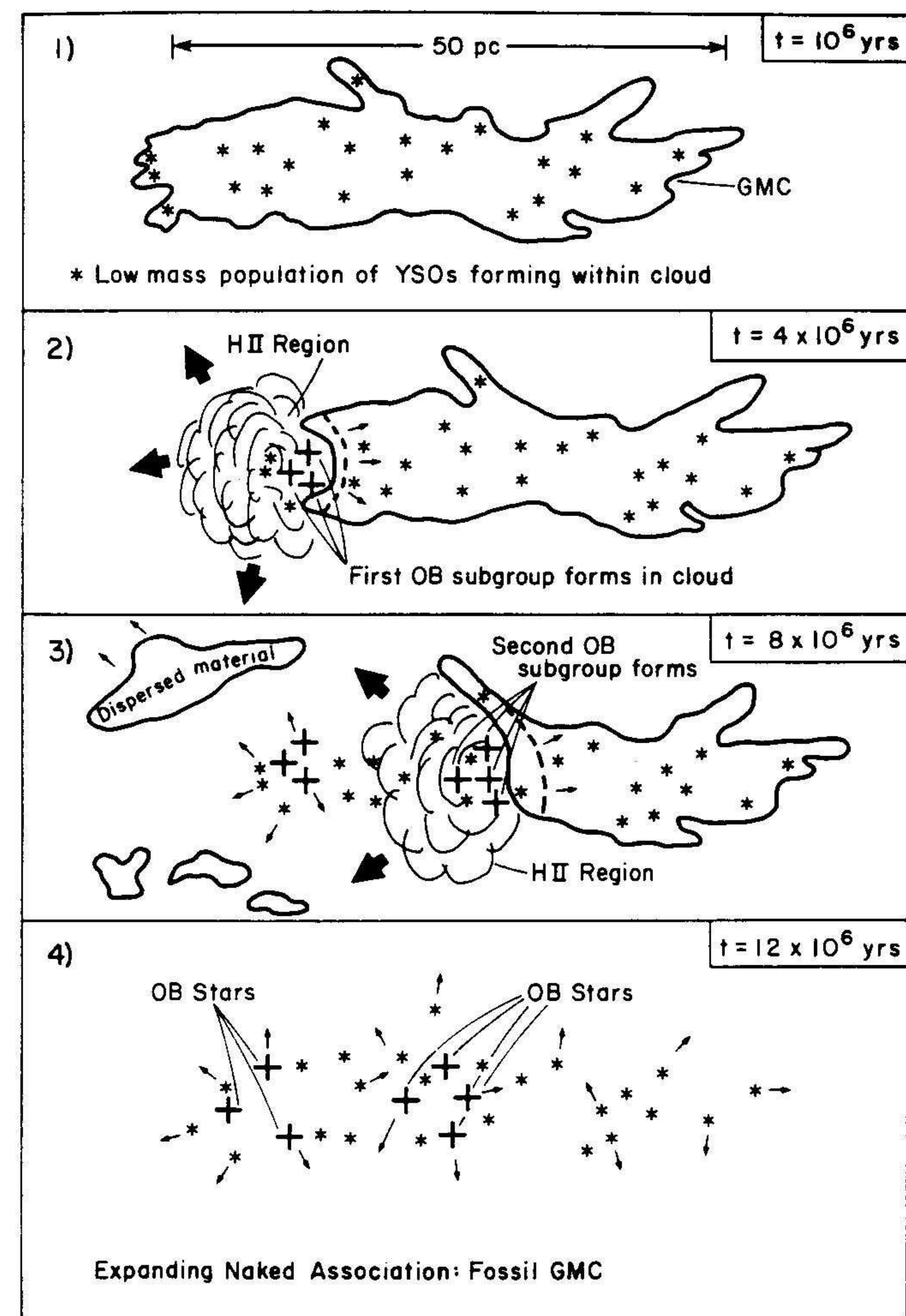


Figure 5: A schematic diagram illustrating the evolution of an OB association. Taken from Lada²⁸.

Physical Properties of A Standard GMC	
Mass	$2 - 3 \times 10^5 M_{\odot}$
Maximum Linear Extent	50-100 pc
Mean Density($n(\text{H}_2)$)	$200-300 \text{ cm}^{-3}$
Mean $N(\text{H}_2)$	$3 - 6 \times 10^{21} \text{ cm}^{-2}$
Typical Linewidth	$2-4 \text{ km s}^{-1}$
Kinetic Temperature	10 K
Sound Speed	0.2 km s^{-1}
Typical Magnetic Field Strength	$30 \mu\text{G}$
Alfven Speed	3 km s^{-1}

which characterize the gas. However, two factors make molecular hydrogen generally unobservable in molecular clouds: first, because it is a homonuclear molecule molecular hydrogen lacks a permanent dipole moment and its rotational transitions are extraordinarily weak; second, it is so light in weight that its lowest rotational transitions are at mid-infrared wavelengths and are too energetic to be collisionally excited at the temperatures that characterize GMCs. Consequently GMCs are best traced by emission lines of molecules such as CO, CS or NH_3 and much of what we know about the physical conditions in GMCs is derived from observations of these molecules.

Molecular emission lines from GMCs are typically characterized by linewidths in the range $2-4 \text{ km s}^{-1}$. Given the masses and sizes of these clouds, their linewidths are close to what one would predict if the clouds are in virial equilibrium, (i.e., $\Delta V \approx (GM/R)^{-0.5}$) which is consistent with the idea that the clouds are bound. At the same time however, the linewidths are considerably greater than that expected for thermal motion of the emitting gas molecules (of mass m):

$$\Delta V_{FWHP} = 2.354(kT/m)^{0.5} = 0.05 \text{ km s}^{-1} \text{ for CO.}$$

This indicates that the overall dynamical state of a GMC is characterized by supersonic, non-thermal, bulk motions. If these motions are turbulent in nature, they should be highly dissipative,²⁴ yet GMCs maintain their supersonic dynamical states throughout their lifetimes, estimated to be on the order of 10^7 to 10^8 years. Although they are gravitationally bound, GMCs cannot be in a state of overall dynamical collapse because the resulting star formation rate ($\sim 250 M_{\odot} \text{ yr}^{-1}$) would be considerably in excess of observed values.²⁵ Moreover, the free-fall time for the collapse of a GMC is short compared to the its lifetime. Therefore it is clear that GMCs are being supported against global dynamical collapse by some mechanism. However, GMCs are too cold to be supported by thermal pressure. Exactly what does support GMCs against collapse has been a long standing problem in star formation research.

Molecular clouds are permeated by magnetic fields with strengths in the range of 10 to $1000 \mu\text{G}$.²⁹ The largest values arise in extremely dense very compact regions which exhibit OH maser emission. More typical field strengths are on the order of

about $30 \mu\text{G}$. The Alfven speed, $v_A = B/(4\pi\rho)^{1/2}$ is therefore about 3 km s^{-1} . Thus the fluid motions within a GMC are sub-Alfvenic and perhaps less dissipative than is suggested by their otherwise supersonic dynamical state. Moreover these field strengths are sufficiently strong that they may retard or prevent the global collapse of a GMC.^{30,31} The typical physical properties of GMCs in the solar neighborhood are summarized in Table 1

3.3. The Structure of GMCs: Dense Cores

The molecular mass of a GMC is spatially distributed in a non-uniform manner. These clouds are highly structured, consisting of numerous filaments, clumps and dense cores.³² In fact GMCs are so complex that it is very difficult to provide a meaningful quantitative description of their structure.³³ Molecular clouds have fractal geometries with a typical fractal dimension of 1.5, but it is not at all obvious what the significance of this fact is.^{34,35} A crude but useful way to characterize molecular cloud structure is to determine the fraction of cloud mass at various densities. The densities in GMCs range from a few hundred to a few million hydrogen molecules per cubic centimeter. Most (80-90%) of the material is at densities between $100-1000 \text{ cm}^{-3}$. About 10 % of the gas is contained in clumps and cores with mean densities of 10^4 cm^{-3} or slightly more. The distribution of dense gas through a GMC is generally not a well determined quantity. However, recent studies of the Orion clouds provide some indication of how such gas might be distributed.^{36,37} Dense gas is traced by molecular transitions whose excited states require high densities to be collisionally populated and which are optically thin. The most extensively used tracers for this purpose have been the the $J=2-1$ line of CS and the (1-1) metastable transition of NH_3 , although other transitions and other lines can be equally useful.

In Figure 6 is displayed the CS($J=2-1$) map of the Orion B molecular cloud.³⁶ Here the regions of brightest CO emission (see Figure 4) have been completely surveyed by Lada, Bally and Stark³⁶ (hereafter LBS) for CS emission. The distribution of the CS emission and the high density gas is very clumpy. Moreover, the map appears to be dominated by a few very large clumps or cores. More than 40 dense cores were identified by LBS within the mapped region. These cores were found to have radii which ranged from 0.1 pc (the limit of telescopic resolution) to 0.5 pc. The cores were typically elongated and not circular in shape with a mean aspect ratio of 2.0 which is similar to dense cores studied in other regions.^{38,39,40} These cores were found to range in mass between 8 - $500 M_{\odot}$. The mass spectrum of these cores is displayed in Figure 7. For cores with masses in excess of $20 M_{\odot}$ LBS found that the spectrum is well represented by a power-law with an index of -1.6. Since the spectral index of the cloud core mass spectrum is greater than -2, most of the dense gas in this GMC is contained in the most massive cores. Indeed, more than 50% of the dense gas detected was found to be contained within the 5 most massive cores.³⁶ In this regard the mass spectra of molecular cloud cores is qualitatively different that that (i.e., $\gamma_* = -2.35$) of stars which presumably form from them.⁴¹ Since the definition of a core is arbitrary one might question the significance of the derived mass spectrum. However, LBS derived the mass spectrum for the Orion B dense gas using two different clump definitions

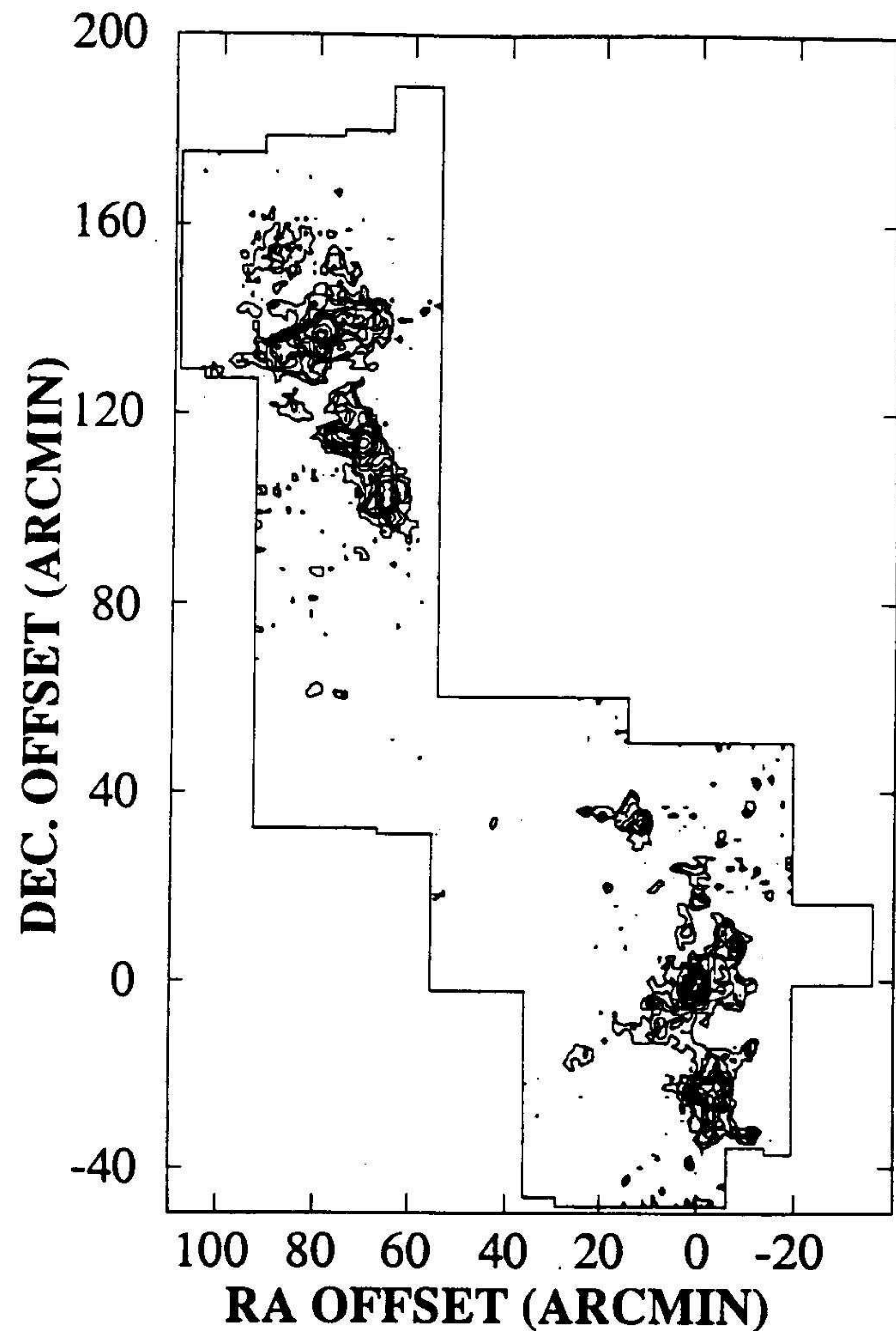


Figure 6: Distribution of dense gas in the L1630 (Ori cloud B, see Figure 4) molecular cloud as traced by CS emission. Taken from LBS³⁶.

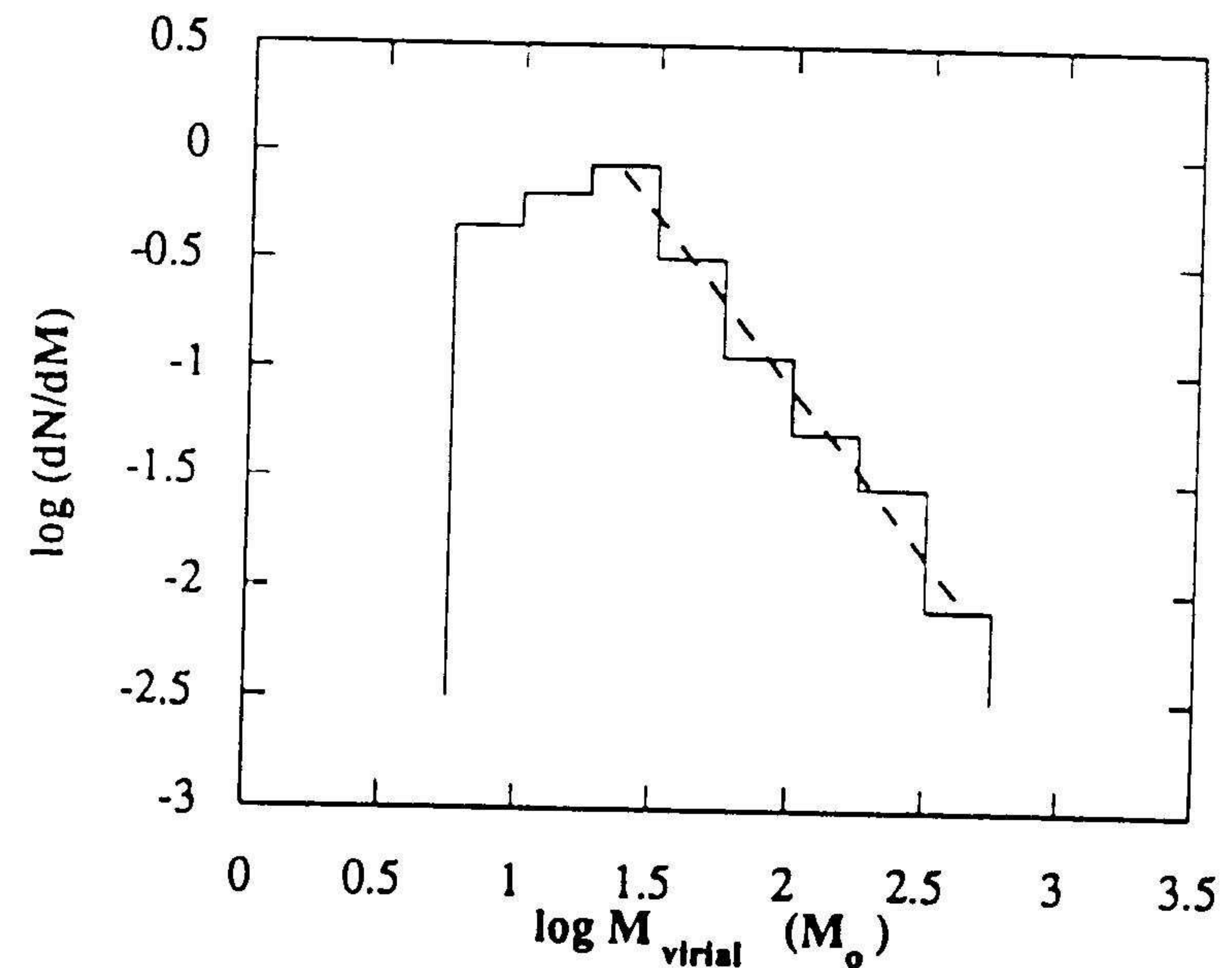


Figure 7: The mass spectrum of dense cores in the L 1630 cloud from the study of LBS³⁶. The spectrum can be characterized by a power law with an index of -1.6.

and got the same result. Moreover, it is interesting that observations of lower density clumps in 5 other GMCs as well as the Orion A cloud yield clump mass spectra with very nearly identical spectral indices despite the fact that different definitions of clumps were employed in each case.^{32,37}

There exists an empirical relationship between the linewidth and the size of cloud cores or clumps when the range of sizes being considered spans 2-3 orders of magnitude (i.e., $R \sim \Delta V^{0.5}$).^{42,32} Although more exotic explanations have been proposed,^{42,44} the most straightforward and likely interpretation of this relation is that the cores and clumps are self-gravitating and in virial equilibrium.⁴³ This is illustrated by Figure 8 which displays the relation between the non-thermal velocity dispersion of a cloud and its size.⁴³ Also plotted are model equilibrium relations for the observed parameters. These models have been calculated with the assumptions that: 1) the cores are in virial equilibrium; 2) they are internally supported by the non-thermal motions which give rise to their supersonic linewidths; and 3) the non-thermal motions are generated by the magnetic waves. The results for three different values of field strength are presented and it is clear that for field strengths typical of GMCs (i.e., $30 \mu\text{G}$) magnetic fields can support the clouds in a state of virial equilibrium. For virial equilibrium, (i.e., $\Delta V \sim (GM/R)^{1/2}$) and a linewidth size relation given by $\Delta V \sim R^{0.5}$, it follows that $M \sim R^2$ (i.e. the column density of the cores is constant)

Physical Properties of Dense Cores	
Masses	5 - 500 M_{\odot}
Mass Spectrum	$f(m) \propto m^{-1.6}$
Radii	0.1-2.0 pc
Aspect Ratio	≈ 2.0
Mean Density ($n(\text{H}_2)$)	10^4 cm^{-3}
Density Structure	$n(r) \sim r^{-1.6}$
Linewidths	0.2-4 km s^{-1}
Kinetic Temperatures	10-20 K

and $M/R^3 \sim R^{-1}$, (i.e., the core density is inversely related to its size). However, it is important to note that the data upon which such conclusions are drawn, are taken from a heterogeneous sample of observations of many different clouds using different molecular tracers. For an individual cloud, in a single tracer, the linewidth size relation can be significantly different in slope⁴² or it may not exist at all³⁶. On the other hand, a clear trend between linewidth and size is apparent for individual cores when they are observed with molecular lines which trace different number densities (e.g., C^{18}O , CS and NH_3).⁴⁵ Such observations indicate again that dense cloud cores are likely bound, virialized and centrally condensed with number density varying inversely with size (i.e., $n(r) \sim R^{-1.6}$).⁴⁵

4. The Young Stellar Objects

4.1. Clustering and Multiplicity

Stars form in GMCs and so in this sense we expect the youngest stars to be found in groups, that is, to be spatially confined to the well defined boundaries of a GMC.²⁸ On the other hand, what one should expect about the spatial distribution of stars within a GMC is not at all obvious. The positions of these stars are essentially the positions of the sites of star formation activity. Knowledge of the spatial distribution of these sites and its relation to other physical properties of a star forming region (e.g., cloud structure, chemistry, temperature, and dynamical state, presence of HII regions, supernova remnants, shocks, winds, etc.) is clearly important for developing a theory of star formation. Unfortunately, stars located within a GMC are heavily extinguished and difficult to observe. As a result, until recently, little was known about the distribution of young stellar objects (YSOs) within molecular clouds. The best (and only) way to get a good census of the stellar content of a GMC is through infrared observations and such observations have been only practical during the last few years. The IRAS satellite provides a data base of completely spatially sampled far-infrared observations of the sky and can be used to obtain flux limited counts of far-infrared sources in nearby clouds. However, the majority of young stars in a cloud are weak far-infrared emitters and cannot generally be detected by IRAS. Moreover,

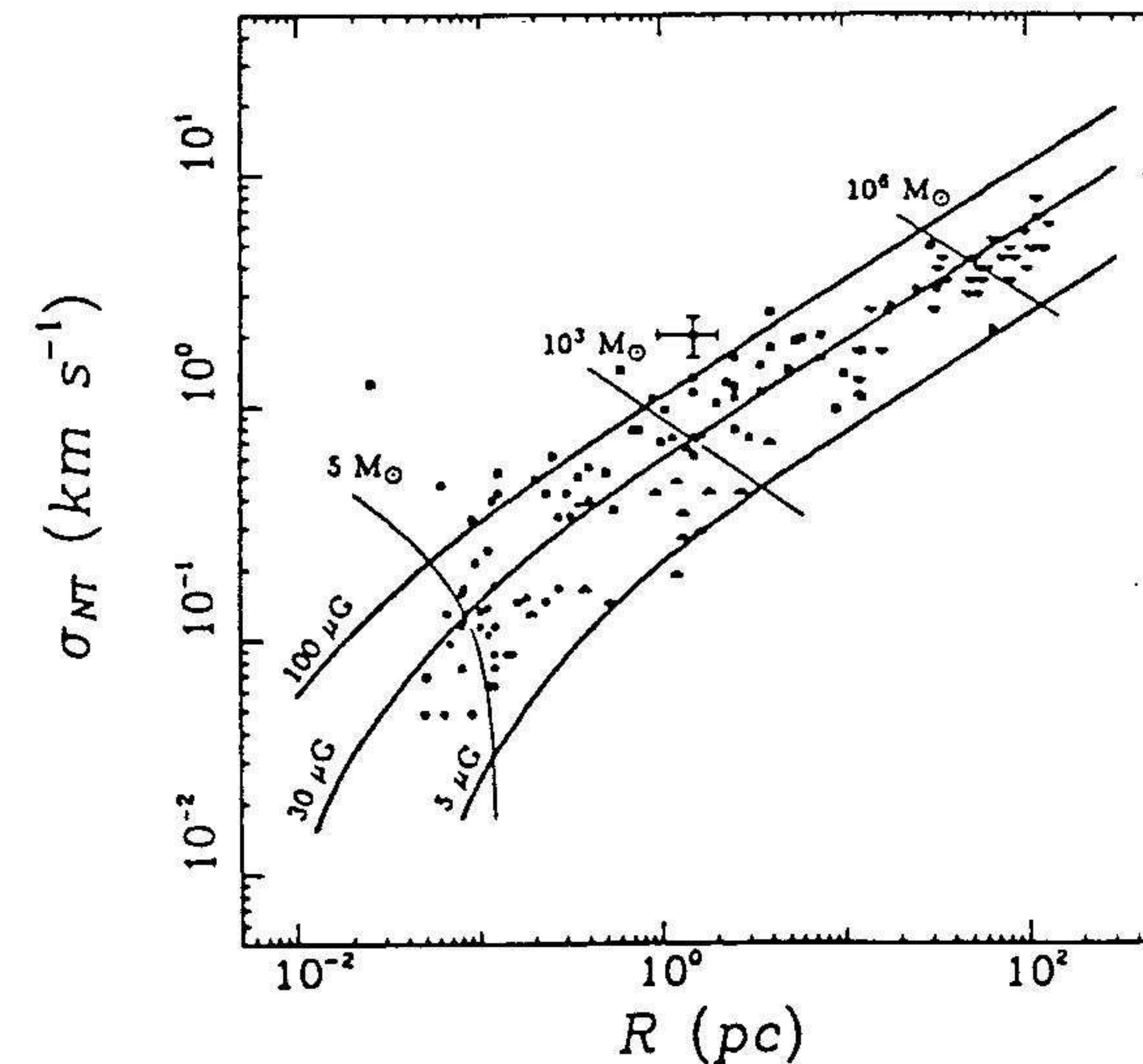


Figure 8: The relation between the size of a cloud its non-thermal velocity dispersion. Also plotted are curves representing the predictions of virial equilibrium models for various magnetic field strengths. From Myers and Goodman⁴³.

the angular resolution of IRAS was relatively coarse so that the results are often compromised by source confusion even in the nearest clouds. Near-infrared imaging surveys are much better suited to detect such stars, although such observations are themselves often limited by background source confusion.

The first cloud to be systematically surveyed at near-infrared wavelengths was the L1630 (Orion B) cloud^{46,47} which makes up the northern half of the Orion GMC complex (see figures 4,6). A large region of the cloud surrounding the all the regions of significant CS emission was observed at $2.2 \mu\text{m}$. Roughly half the area surveyed contained CS emission and dense gas. The observations were sensitive enough to observe a large span of the IMF and most of the stars observed had masses comparable to or less than that of the sun. The spatial distribution of these stars showed a strong tendency for the stars to be clustered. More than half ($\sim 58\%$) of all the infrared sources detected were found to be contained within three rich clusters which together subtended an angular size less than 18% of the entire area surveyed. After correcting for the presence of background/foreground star contamination, it was found that 96% of the sources *physically associated* with the cloud were contained in these 3 clusters. Figure 9 shows the relation of the clusters to the dense gas in the cloud. The three rich clusters are spatially associated with 3 of the 5 most massive dense cores in the cloud.⁴⁷ These observations vividly demonstrate that in this cloud star formation occurs almost exclusively in: 1) rich clusters and 2) dense molecular gas. Indeed, the first phenomenon likely follows from the second. That is, if dense gas is a necessary

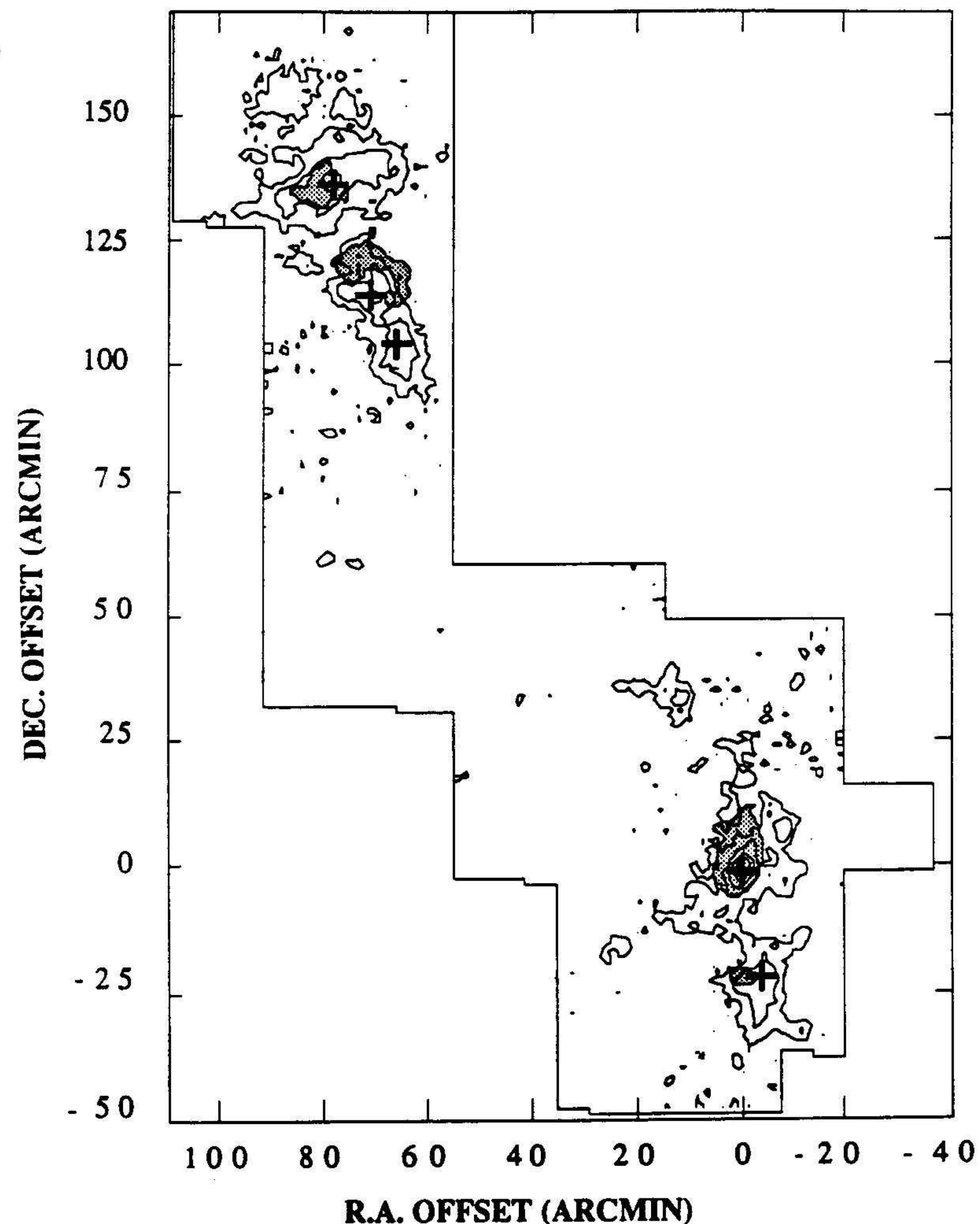


Figure 9: The locations and extents of four embedded infrared clusters (shaded contours) compared to the distribution of dense molecular gas (solid contours) in the L1630 cloud. Figure from Lada⁴⁷.

condition for star formation then we expect most stars to form in a few rich clusters. This follows because the mass spectrum of dense gas in the cloud indicates that most of the dense gas is contained in the few most massive cores. The fact that two of the massive cores in L1630 did not produce rich clusters indicates that although dense gas may be a necessary condition for star formation it is not a sufficient condition for star formation.

Since the core mass spectra of nearby GMCs are so similar, we also expect that these clouds should also produce most of their stars in embedded clusters as well. Indeed, infrared imaging observations have uncovered rich embedded clusters in almost every GMC studied,⁵⁰ although in these additional cases the observations are not extensive enough to determine whether clusters account for the bulk of all stars formed. An exceptional case is the λ Ori OB association, a fossil association which has recently emerged from and cleared away its parental GMC.²⁶ A systematic survey of emission line stars over the entire association shows that the majority of stars detected are also clustered²⁶. The clusters are about a factor of 4 more extended than those in L1630. However, these sizes are what would be expected if the clusters started out with dimensions similar to those of L1630 (i.e., 1 pc) but became unbound after gas removal from the association (i.e., the velocity dispersion of stars in the association is measured to be $\sim 2 \text{ km s}^{-1}$ and the age of the OB cluster in its center is about 3×10^6 years^{48,49}).

On the other hand, observations of the L1641 cloud (the Orion A cloud) present a somewhat different picture for that cloud. A spatially complete emission line survey⁵¹ and an extensive (but not spatially complete) infrared survey⁵² of the cloud suggest that in addition to stars forming in rich embedded clusters and small groups there is a more distributed population of stars which could account for as much as half of all stars formed in the cloud. The origin of this distributed population is at present unclear. However, such observations have given rise to the idea that there are two modes of star formation: a clustered mode and an isolated or distributed mode.^{41,53} In the latter circumstance, individual stars (primarily low mass stars) are formed in individual low mass cores distributed throughout a molecular cloud.²⁸ The prototypical example of the isolated mode of star formation is the Taurus complex. With a mass of $\sim 10^4 M_{\odot}$, the Taurus dark cloud is a relatively small molecular cloud complex. The complex consists of a number of filamentary structures which contain small dense cores. These dense cores span a small range of the clump mass spectrum from about 1–40 M_{\odot} . About half of these cores contain newly formed stars³⁹ but typically there is only one star within an individual core. However, even in this case careful analysis of the spatial distribution of stars indicate that most stars form in loose groups rather than in complete isolation. Statistical analysis of the members of this T association shows that most of the stars in the cloud have companions which formed within a distance of order the size of a typical cloud core.⁵⁴ Indeed most of the known members of the association were found to be members of 6 identified clusters. This is illustrated in Figure 10. These clusters differ from those in L1630 primarily in their richness. It is interesting to note in this regard that similar poor clusters have been found throughout the Orion A (L1641) cloud in an imaging survey of the IRAS

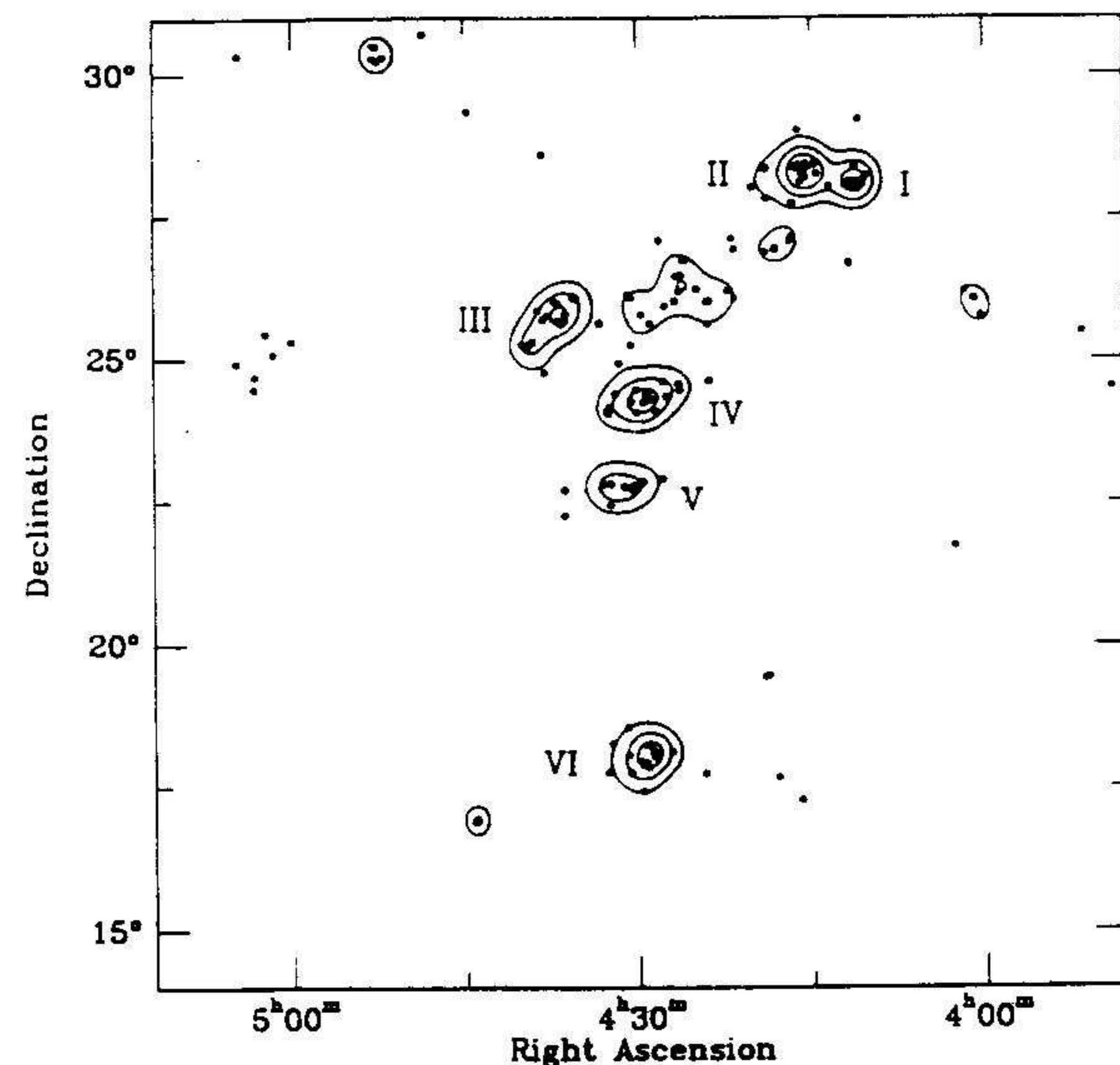


Figure 10: Contour maps marking the locations of groupings of YSOs in the Taurus molecular cloud as identified by Gomez *et al.*⁵⁴ Positions of the YSOs are also indicated.

sources in that cloud.⁵⁵ These observations may suggest that stars form in groups with a spectrum of richness from relatively poor clusters (stellar density enhancements⁵⁵) with only a few stars to very rich clusters with hundreds of stars. Again, to the extent that the (stellar) mass spectra of clusters follow the mass spectra of cores from which they form, we would expect most stars in a GMC to originate in relatively rich clusters rather than in poor clusters or in isolation. We note here that most of the rich clusters that form in GMCs must be disrupted soon after they emerge from the cloud, otherwise there would be considerably more (bound) open clusters in the field than are observed.³ This suggests that the star formation efficiency in cluster forming cores rarely reaches values as high as 50%.^{3,56}

As is the case for field stars, there is a high frequency of multiplicity, namely binarity, among pre-main sequence stars. Indeed, for stars in the Taurus T association the binary frequency is found to be higher (perhaps by a factor of 3) in the mass range surveyed than it is in the field.^{57,58} At the same time a study of the binary stars in the very rich Trapezium cluster indicates a binary population very similar to the field.⁵⁹ These results confirm the field star results that most stars form in binary systems. They also suggest that most field stars were formed in environments typical of rich clusters like the Trapezium rather than in poor groups such as in Taurus. It is possible that binaries form at the same frequency both in clusters and in isolation,

but in the environment of a rich cluster many binaries become disrupted very early in their evolution, while those formed in relative isolation survive for longer times.

In summary, most stars appear to have been formed in binaries within either rich clusters or small stellar groups.

4.2. The Initial Luminosity Function

The field star IMF is a globally averaged quantity, averaged over both the lifetime of the galaxy and over a specific volume of space (i.e., the solar neighborhood). Although it is often assumed that the IMF is universal in both time and space, this has never been demonstrated in a completely satisfactory way. However, in order to develop comprehensive theories for star formation and galactic evolution it is crucial to know whether the detailed form of the IMF is universal. Are there spatial and/or temporal variations in the initial conditions and other important astrophysical parameters that can alter the process of star formation and the form of the IMF? Or is star formation such a robust process that the outcome is always an IMF of the same form?

In principle, observation of large enough groups of young or newly forming stars in different parts of the galaxy should be able to provide fundamental constraints on these questions. The smallest spatial size scale over which a meaningful determination of a luminosity function can be made is that characteristic of an open cluster. Clusters are important laboratories for studying the initial luminosity function because they consist of statistically significant groups of stars who share the common heritage of forming from the same parental cloud at the same epoch in time. Young embedded clusters are particularly useful since they are not old enough to have lost significant numbers of members due to stellar evolution or dynamical effects such as evaporation or violent relaxation.^{56,3} However, study of very young clusters suffers from two disadvantages: 1) the clusters are often heavily obscured and cannot be easily observed at optical wavelengths; 2) the stars in such a cluster are mostly pre-main sequence stars and uncertain corrections for pre-main sequence evolution and non-coevality must be applied to the members to derive mass spectra from luminosity functions. Only in the last few years have advances in infrared detectors enabled the direct observation of such embedded and often obscured clusters and helped to minimize the first disadvantage. The second disadvantage requires modeling and is more difficult to overcome.^{50,60,61}

Figure 11 shows the K-band ($2.2\mu\text{m}$) luminosity function (KLF) of the cluster IC 348 in Perseus.⁶¹ This luminosity function illustrates two important features shared by the infrared luminosity functions of most young clusters: First, the KLF appears to be power-law in form for the brightest stars; Second, the shape of the KLF departs from a power-law at large (faint) magnitudes consistent with a flattening or turn over at the lowest stellar luminosities. The slope of the power-law portion of the KLF of IC 348 has a value of $0.40 (\pm 0.03)$. This is very similar to the slopes of the power-law portions of the KLFs measured for the other young clusters in nearby GMCs (i.e., 3.2-3.8).^{36,62} The breadths of young cluster KLFs and therefore the location of their points of departure from the power-law form appear to differ. For example, the KLF

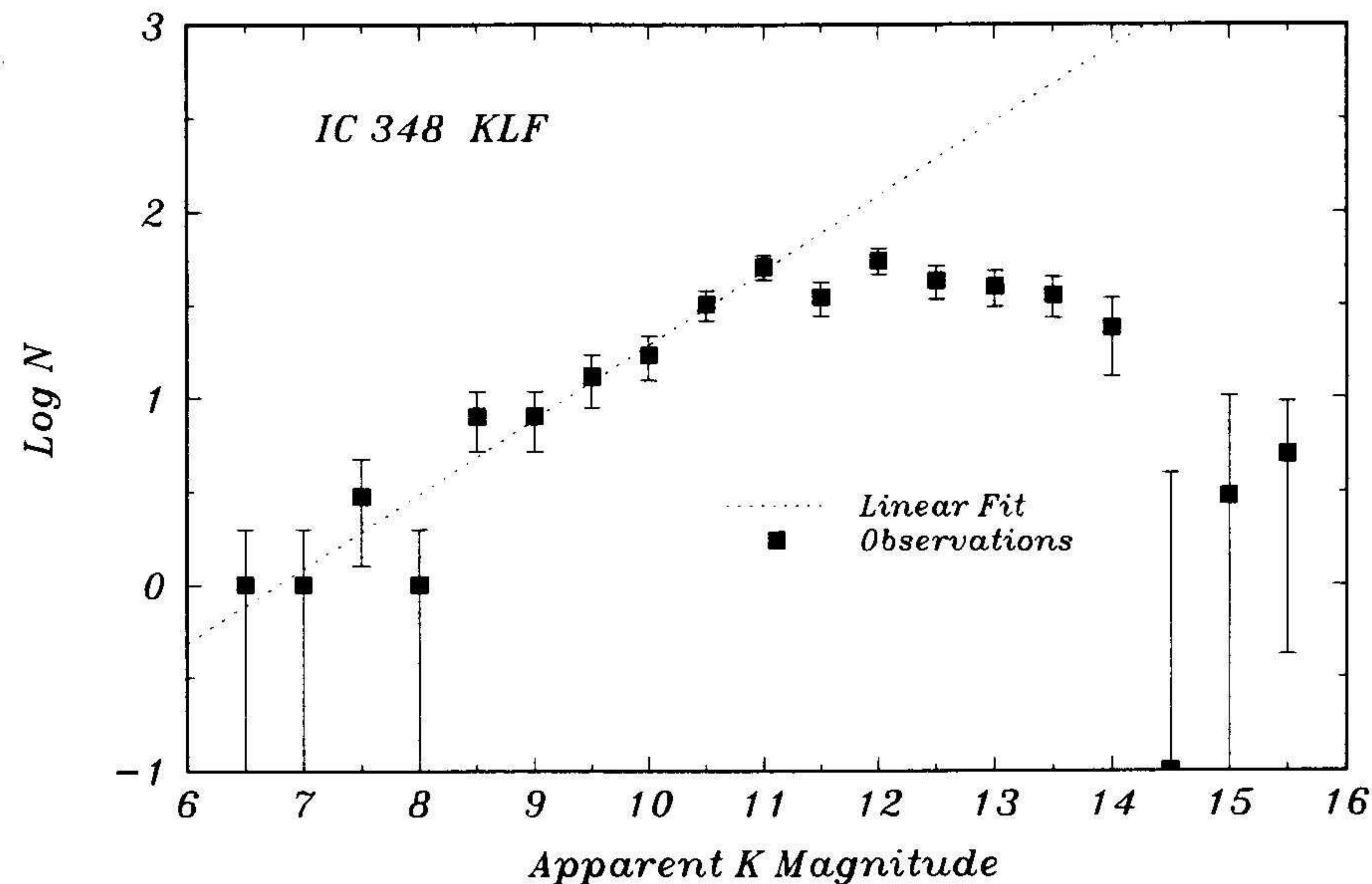


Figure 11: The K band luminosity function of the young cluster IC348 in Perseus. (From Lada and Lada⁶¹).

of the Trapezium cluster⁵⁰ is significantly narrower than that of IC 348.⁶¹

The luminosity function of a very young cluster is closely related to its initial mass function. For a stellar system for which the mass function and mass-luminosity relation are power law in form (i.e., $dN(\log m_*) \propto m_*^{-\gamma} d\log m_*$; $L_K \propto m_*^\beta$), the slope of the K luminosity function can be shown to be:

$$\alpha = \frac{\gamma}{2.5\beta}$$

Here γ and β are the spectral indices of the stellar mass function and the K luminosity-stellar mass relation, respectively. For early-type (O-F) *main sequence* stars which are sufficiently hot that their infrared emission is in the Rayleigh-Jeans regime, one can show that the K luminosity-mass relation is approximately a power law with $\beta = 2.0$ and consequently $\alpha = \frac{\gamma}{5}$. For an underlying mass function similar to that derived for local field stars by Salpeter¹³ $\gamma = 1.35$, and $\alpha = 0.26$. This appears to be significantly flatter than the slopes derived for the bright end of the KLFs of most young clusters. There are two reasons for this: 1) a single power-law shape is not consistent with the functional form of the field star IMF at all stellar masses and 2) there is not a unique mass-luminosity relation for pre-main sequence stars (which are mostly on convective tracks in the HR diagram) as there is for main sequence stars. The latter is the most important factor. The luminosities of a group of PMS stars depend on both the masses of the stars and the amount of time that has expired since

they first appeared on the birthline. A further complication arises if the cluster is not coeval, that is if the age of the cluster is comparable to duration of star formation in the core within which it is forming. To account for all these effects requires modeling. Such modeling indicates that β is a strong function of time for a coeval cluster and the high degree of observed similarity of the power-law portions of young cluster KLFs arises as a consequence of the superposition of non-coeval episodes of star formation in clusters.⁶¹ The breadth of the KLF also turns out to be a function of cluster age and the duration of star formation, the older the cluster or the longer the duration of star formation the broader the KLF. Most importantly, perhaps, the results of such modeling suggest that all young clusters have KLFs that are consistent with the notion that these clusters are characterized by the same underlying IMF, the IMF of field stars. There is as yet no compelling evidence from observations of young clusters in nearby GMCs to suggest that the IMF has significantly varied in either time or space.

4.3. The Nature and Evolutionary Status of Young Stellar Objects

Determining the nature of young stellar objects is essential to deciphering their evolutionary states and developing a theoretical understanding of star formation. The evolutionary status of a normal star is essentially determined by its placement on the HR diagram which requires measurements of two quantities: luminosity and effective temperature. It is therefore no surprise that stars are most usefully classified by these two parameters (i.e., spectral type and luminosity class). The luminosity of a star is straightforwardly determined from its observed flux and its distance. The effective temperature of a star is determined from its colors or observations of temperature sensitive spectral features. This method works very well as long as a star is well behaved spectrally, that is, as long as it produces a black-body like spectrum and can be characterized by a single effective temperature. However, in this sense most young stellar objects are not normal stars. A good example is the famous young star FU Ori. The spectral type of this star is a function of the wavelength at which it is observed. Consequently, FU Ori cannot be characterized by a single effective temperature. Its placement on the HR diagram is ambiguous and the classical theory of stellar evolution cannot explain its nature.

This "abnormal" characteristic of young stellar objects is a result of their intimate physical association with the natal gas and dust from which they are formed. New stars are born within dense molecular cloud cores and throughout their formation and early evolution they are associated with varying amounts of molecular gas and dust. This circumstellar gas and dust can absorb and reprocess substantial amounts of the radiation emitted by the embedded stars significantly altering their spectral appearance. Indeed, at optical wavelengths the youngest objects are rendered completely invisible by the obscuration of opaque circumstellar dust and a significant fraction, if not all, of their luminous energy is radiated in the infrared portion of the spectrum. In general the circumstellar gas and dust associated with young stellar objects has a spatial extent considerably greater than that of a stellar photosphere. Consequently,

emitting circumstellar dust, which is in radiative equilibrium with the stellar radiation field of the buried star, will exhibit a wide range of (effective) temperatures and the emission that emerges will have a spectral distribution much wider than that of a single temperature blackbody. For this reason it can be very difficult, if not impossible, to meaningfully place a YSO on an HR diagram.

Clearly, the evolutionary status of a young stellar object cannot be derived solely from knowledge of its luminosity or a single effective temperature. More complete knowledge of its spectrum, particularly at infrared wavelengths, is required. The shape of the broad-band infrared spectrum of a young stellar object depends both on the *nature* and *distribution* of the surrounding material. Clearly then, we expect that the shape of the spectrum will be a function of the state of evolution of a YSO. The earliest (protostellar) stages, during which an embryonic star is surrounded by large amounts of infalling circumstellar matter, should have a very different infrared signature than the more advanced (pre-main sequence and main sequence) stages, where most of the original star forming material has already been incorporated into the young star itself. Observations of low mass young stellar objects have confirmed this expectation and such young stellar objects can be meaningfully classified by the *shapes* of their optical-infrared spectral energy distributions.²⁸

The spectral energy distributions of the vast majority of known (low mass) young stellar objects fall into one of three broad classes designated I, II and III. Figure 12 illustrates spectral energy distributions (SEDs) representing each of these classes. The basic properties of these SED classes and the sources that produce them can be summarized as follows:

Class I Sources: Class I SEDs are broader than a single blackbody function and peak at far-infrared or sub-millimeter wavelengths. Longward of two microns these SEDs usually rise with increasing wavelength producing a huge "excess" of infrared emission compared to that expected from a normal stellar photosphere. They typically exhibit the silicate absorption feature at 10 microns wavelength. Class I sources derive their large infrared excesses from the presence of large amounts of circumstellar dust. These sources are usually deeply embedded in dense molecular cloud cores and rarely exhibit detectable emission in the optical portion of the spectrum. They frequently are associated with small (infrared) reflection nebulae and are often the driving sources of bipolar molecular outflows. Class I SEDs have been successfully modeled as embryonic stellar cores surrounded by circumstellar disks and massive envelopes of gas and dust whose density structure is the same as that predicted for rotating, infalling protostellar cloud cores.⁶³ Figure 13 shows the SED of the Class I source L1551 along with protostellar models for the object. Class I sources are relatively rare among young stellar objects in molecular clouds and statistical arguments suggest ages of these sources of order $1-5 \times 10^5$ years.^{67,68,69}

The identification of protostars is fundamental to the eventual development of a theory of star formation. However, whether or not Class I objects are true protostars in the sense that they are *objects in the process of accumulating into a stellar-like configuration the bulk of the material they will ultimately contain as main sequence*

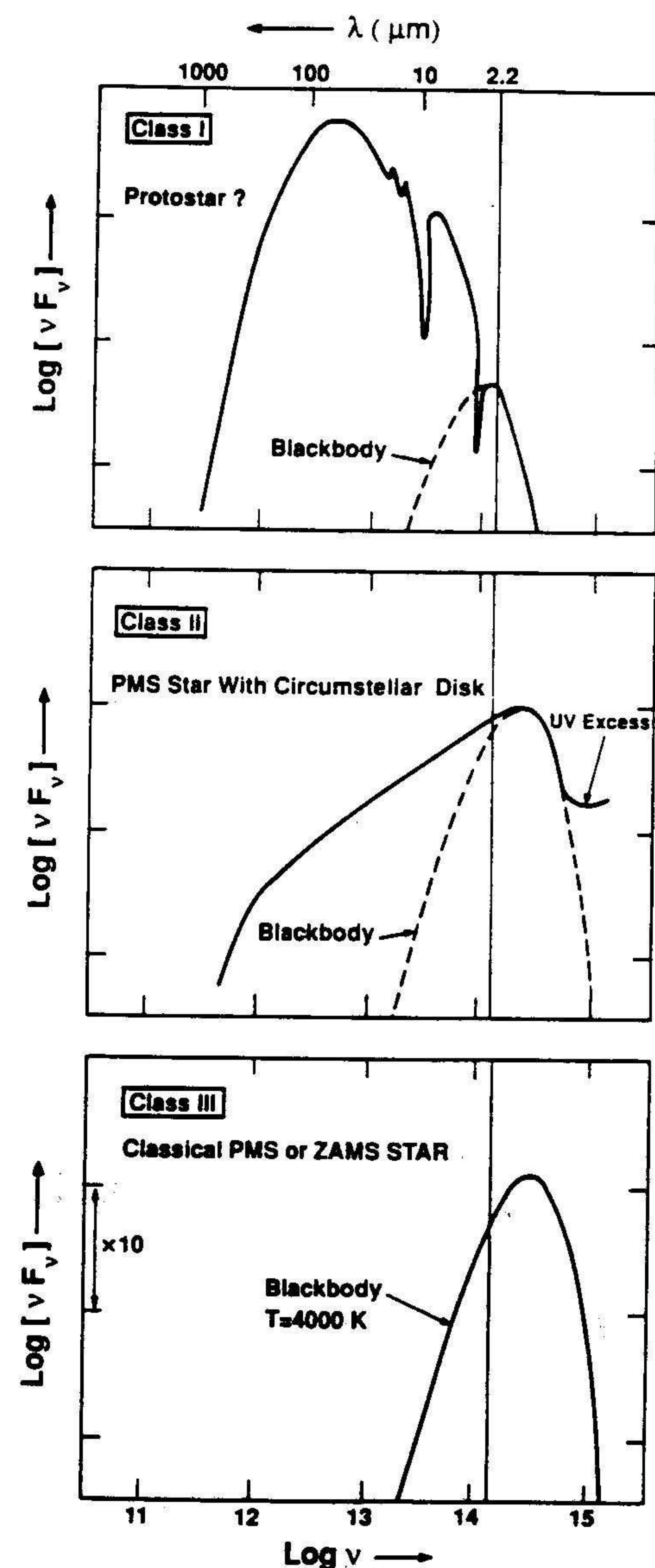


Figure 12: Classification Scheme for YSO spectral energy distributions

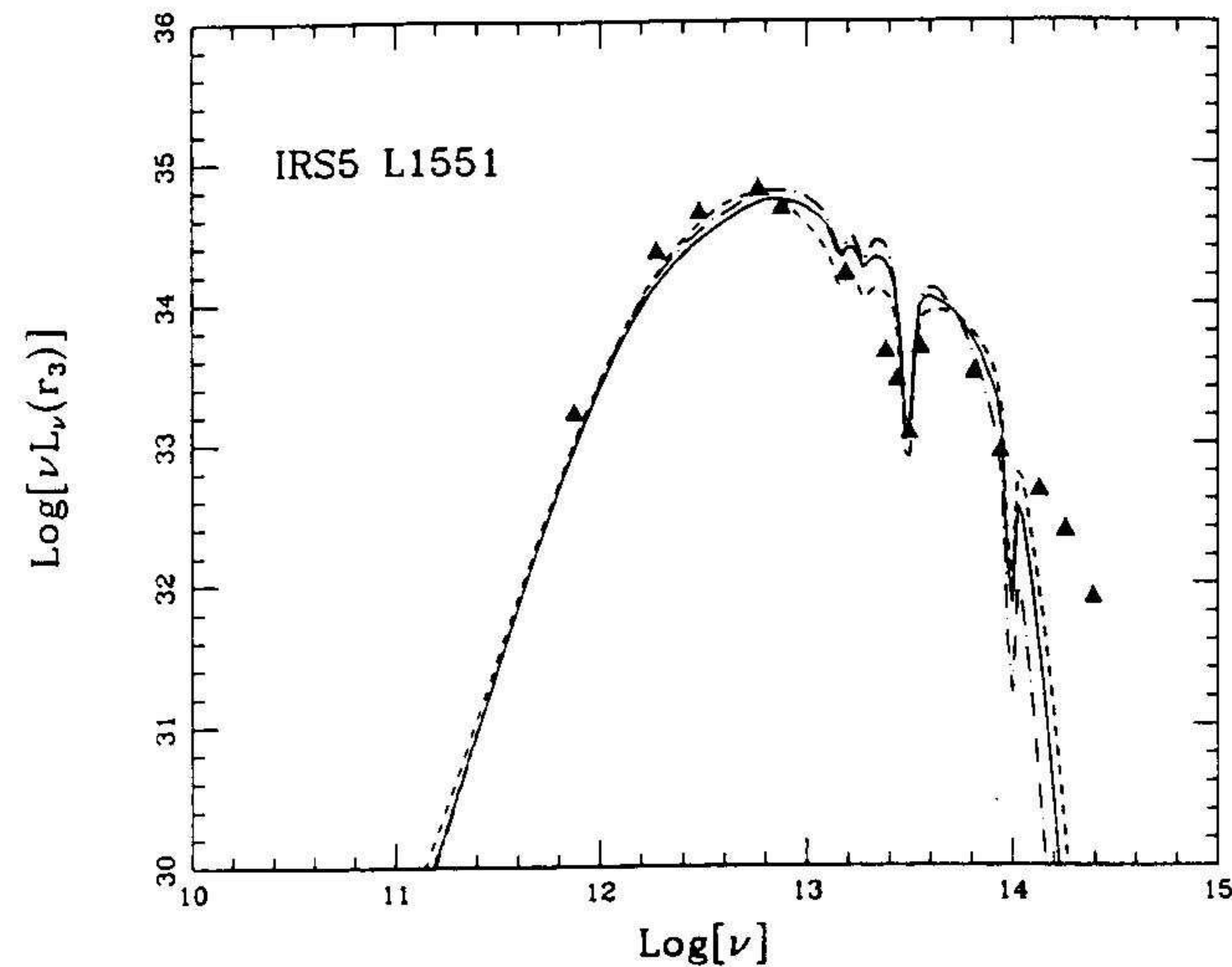


Figure 13: SED for the Class I source L 1551 IRS 5, a protostellar source in the Taurus molecular cloud. Solid and dashed lines show various rotating-collapsing isothermal protostellar models fit to the data. (From Adams, Lada and Shu⁶³).

stars has not been unambiguously demonstrated. Such a demonstration requires the direct detection of infall or collapse motions. A kinematic signature of infall would provide conclusive and compelling evidence that an object or group of objects was truly protostellar. Despite many attempts, detection of such motions around Class I (or any other young) objects has proved elusive. Indeed, as will be discussed below, the circumstellar gas around Class I sources usually provides kinematic signatures of outflow rather than infall motions! There are three known objects for which the line profiles of density sensitive molecules (e.g., CS) exhibit signatures consistent with infall motions of just the right magnitude to be consistent with protostellar theory. These objects are B335,⁸⁴ IRAS 1629⁸⁵ and HL Tau.⁸⁷ Unfortunately, in none of these cases has it been demonstrated that an infall model is a unique explanation of the molecular line observations (although infrared observations of molecular carbon absorption lines in HL Tau appears to provide strong corroborative evidence for infall motions in that source⁸⁶).

Class II Sources: Class II SEDs are also broader than a single blackbody function, however, these SEDs peak at visible or near-infrared wavelengths. Longward of two microns Class II SEDs fall with increasing wavelength usually in a power-law like fashion.^{64,65,66} This results in an infrared excess which, though significant, is much smaller than that exhibited by Class I sources. Therefore, these sources must be surrounded by considerably less gas and dust than Class I objects. Figure 14 shows

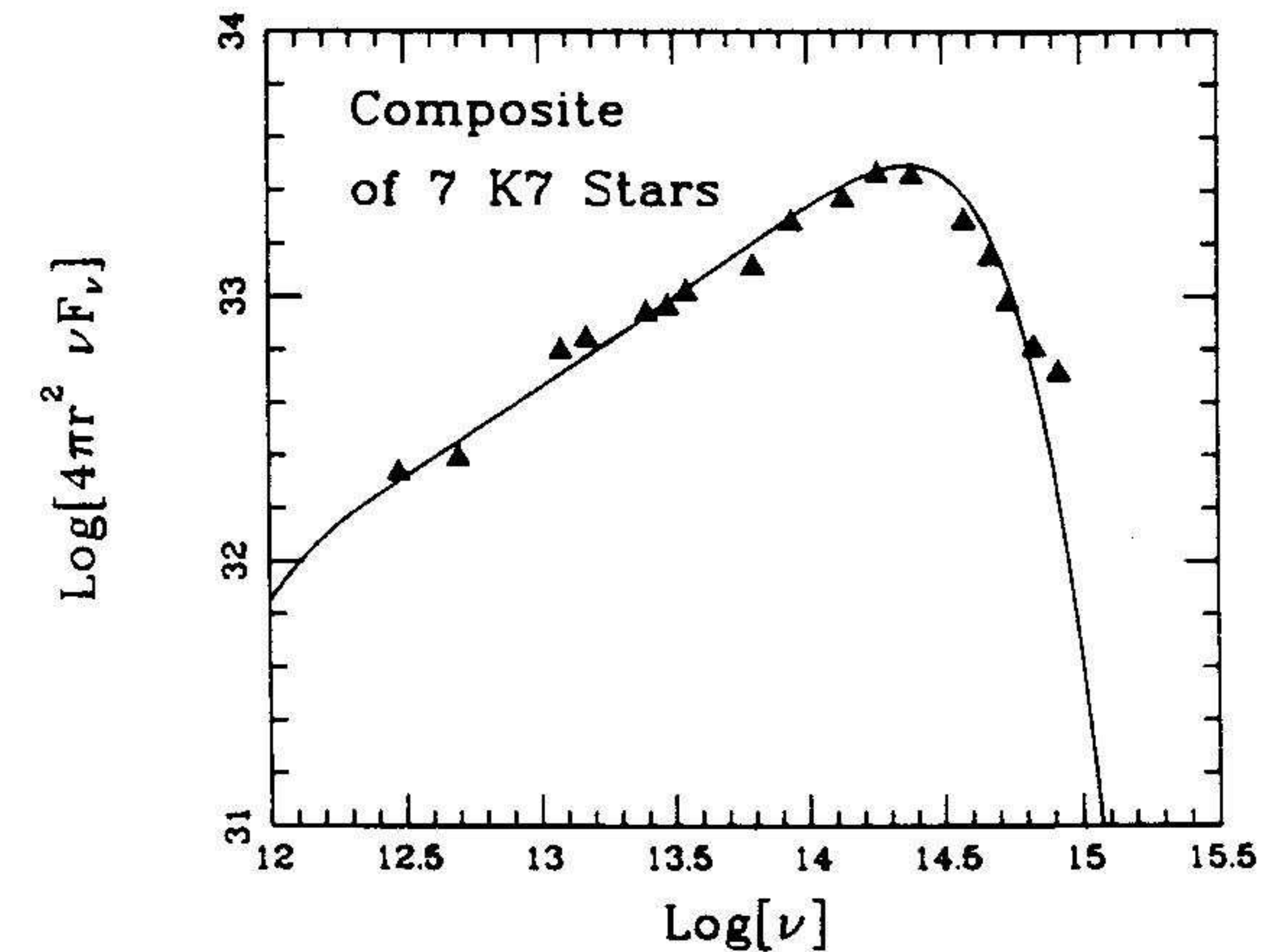


Figure 14: The composite SED of seven Class II stars along with that (solid line) of a model circumstellar disk. (From Adams, Lada and Shu⁶⁶).

the composite SED of seven Class II sources. The dereddened and averaged data points are indicated by triangles and a theoretical fit to the spectrum (in which the infrared portion is modeled by a power-law function) is indicated by a solid curve.

More than a decade ago Lynden-Bell and Pringle⁷⁰ predicted that T Tauri stars would display such energy distributions if they were surrounded by luminous accretion disks. Consider an optically thick and spatially thin disk that surrounds a young star and radiates everywhere like a blackbody. Imagine the disk to be composed of concentric annuli as illustrated in Figure 15 with radial dimension ΔR and area $2\pi R\Delta R$. Each annulus radiates as a blackbody of temperature $T(R)$. The emergent spectrum of the disk will then be the superposition of a series of blackbody curves of varying $T(R)$ as shown in Figure 15. Now if $T(R) \sim R^{-n}$, the Wien laws tells us that the frequency of maximum emission scales as $\nu \sim T(R) \sim R^{-n}$. The luminosity radiated in each annulus is given by:

$$L_\nu d\nu = 2\pi R dR \sigma T(R)^4 \sim R^{2-3n} d\nu \sim \nu^{3-\frac{2}{n}}$$

Therefore, if the temperature gradient in the disk is characterized by a radial power-law, the emergent spectrum will also be characterized by a power-law slope in frequency or wavelength. For an SED, $\nu L_\nu \sim \nu^{4-\frac{2}{n}}$ or $\alpha = \frac{2}{n} - 4$ where α is the slope of the SED when plotted as a function of $\log \lambda$.

Thus the power-law shape of the infrared portion of Class II SEDs strongly suggests that the infrared excess arises in an optically thick circumstellar disk. The slope of the SED is directly related to the temperature gradient in the disk. The slopes of Class II SEDs longward of 2 microns wavelength are observed to have values in the range between -0.7 and -1.3 corresponding to a range in n , the index of the disk

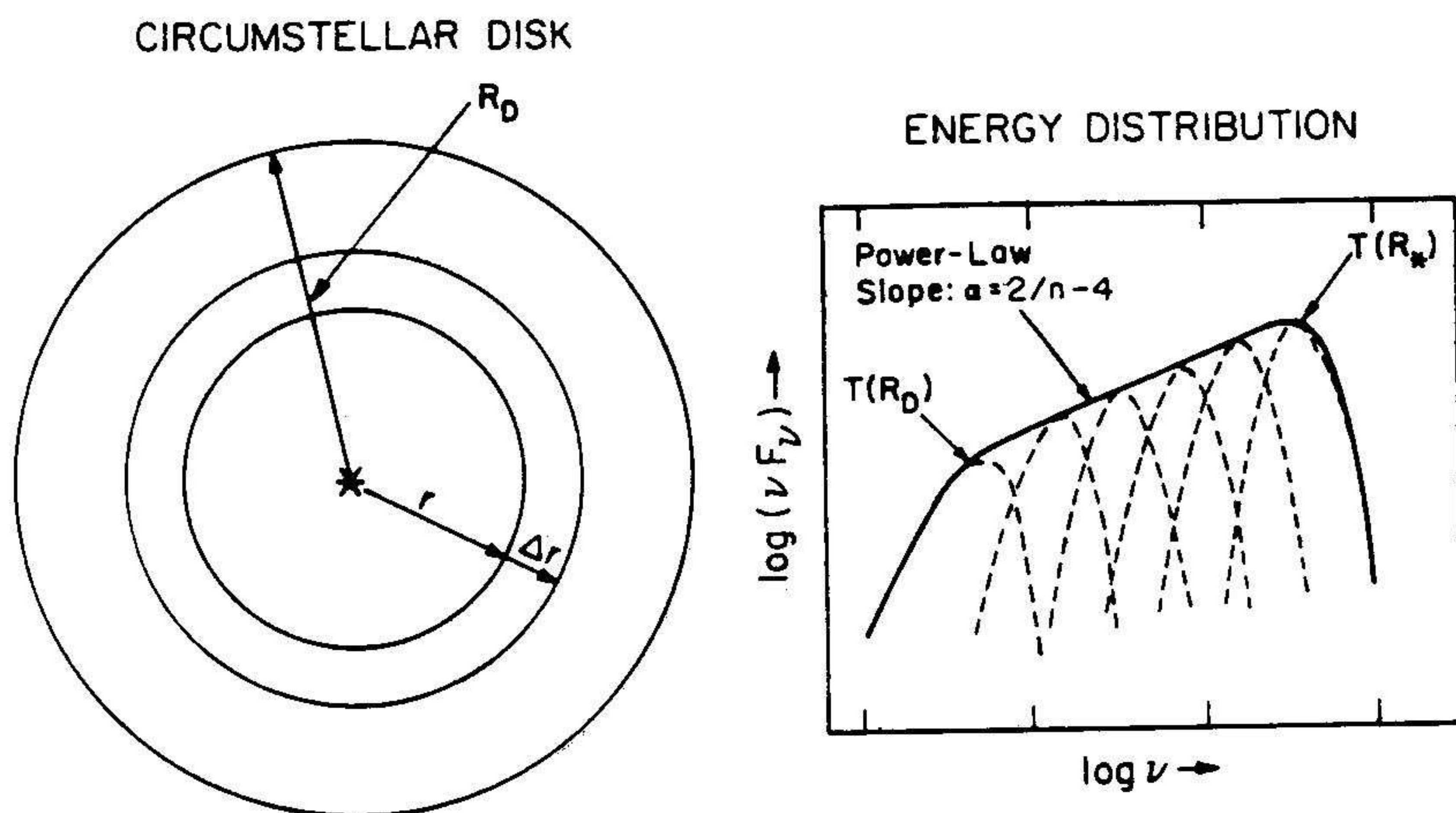


Figure 15: Schematic diagram of a spatially thin, optically thick disk and its emergent spectral energy distribution. The disk spectrum is composed of a superposition of blackbodies of varying temperature.

temperature gradient, of 0.6 to 0.75. A viscous accretion disk is predicted to produce a temperature gradient characterized by $n = 0.75^{70}$ which corresponds to $\alpha = -1.33$. This also turns out to be the same temperature gradient and spectral slope predicted for a flat purely passive disk which derives its luminosity from the reprocessing and re-radiation of light it has absorbed from the central star.^{71,72} The majority of Class II sources have shallower slopes (typically $\alpha \approx -0.7$) which suggests that they are surrounded by flared (passive) disks.⁷³ The excellent agreement between the predictions of disk models and observations as indicated in Figure 14 suggests that the most likely interpretation of the nature of Class II sources is that they represent young stars surrounded by circumstellar disks. They differ from Class I objects in that they lack large, massive (infalling) envelopes of gas and dust. However, it is interesting to note that the infrared to millimeter excess emission from Class II sources is sufficiently large that if the emitting material were spherically distributed and not confined to a highly flattened structure, such as a disk, the star would suffer significantly more extinction than is observed.^{63,74} Indeed, disk masses derived from detection of optically thin continuum millimeter-wave emission range between 0.01–0.1 solar masses.⁷⁴

Class II sources can be observed at optical as well as infrared wavelengths. Therefore, considerably more is known about the nature of these objects than is known about Class I sources. When observed optically Class II sources typically exhibit the characteristics of Classical T Tauri stars (CTTS). Conversely, most all CTTS stars possess Class II SEDs. Classical T Tauri stars are low mass, pre-main sequence, emission-line variable stars. In addition to excess infrared continuum emission, these

stars also exhibit excess emission at ultra-violet wavelengths. The optical spectra of CTTS contain Hydrogen emission lines and frequently various forbidden emission lines as well. The forbidden lines are believed to arise in stellar winds originating near the surface of the star. Typically these lines are observed to be blue-shifted and the absence of red-shifted emission is interpreted as strong supporting evidence for the presence of an occulting disk close to the stellar surface.^{76,77} The origin of the Balmer emission lines is more mysterious. Analysis of these lines provides evidence for both mass loss and mass accretion in these objects.⁷⁵ However, both the mass accretion and ultra-violet excess are believed to be consequences of disk accretion onto the stars.⁷⁵ Because they are visible, CTTS can be placed on the HR diagram, and when their positions are compared to theoretical PMS tracks one derives ages for CTTS usually between 10^6 and 4×10^6 years. However, because the theoretical tracks are calculated assuming diskless PMS stars, it is not clear how they actually relate to the positions of CTTS on the HR diagram. Class II sources are relatively common in star formation regions where they typically outnumber Class I sources by more than 10-to-1.

In summary, Class II sources have been observed over three decades in frequency and over this entire range their SEDs are well matched by the predictions of model stars with circumstellar disks. UV observations and optical spectral-line observations provide additional supporting evidence for the presence of such circumstellar disks.

Class III Sources: Class III SEDs typically peak at visible and infrared wavelengths for low mass stars and decrease longward of two microns more steeply than Class II sources. Since their shapes are more or less similar to single temperature blackbodies, the energy distributions of Class III sources are easily interpreted as arising from extinguished or unextinguished photospheres of young stars. By definition these stars display no infrared excess. However, their light still could be substantially extinguished by foreground dust. Extinction attenuates the spectrum of a YSO by a factor of $\exp(-\tau_\nu)$ and since $\tau_\nu \sim \nu$, for interstellar dust, then $F_\nu \sim \exp(-\nu)$ and it is difficult to distinguish such a spectrum from the high frequency side of a blackbody function where $F_\nu \sim \exp(-\frac{h}{kT}\nu)$. Thus an extinguished star has an energy distribution similar to a blackbody but with the high frequency end exponentially extinguished and the peak displaced toward lower frequencies thus giving the appearance of being "reddened". Low mass Class III sources are typically pre-main sequence stars and by definition are Naked T-Tauri stars (NTTS). They are basically free of any significant amounts of circumstellar gas and dust. Such stars can be thought of as "classical" pre-main sequence stars in the sense that they can be readily placed on the HR diagram and compared to predictions of theoretical PMS tracks.⁷⁸ Comparison with such theoretical tracks shows that the ages of Class III sources range from roughly 10^6 years to more than 10^7 years. Although most Class III sources (NTTS) have ages $> 5 \times 10^6$ years, and are likely candidates for post-T Tauri stars (PTTS), a significant number have ages which overlap with those of CTTS.⁷⁸ Since they lack infrared and ultra-violet excesses, these stars are difficult to distinguish from foreground and background stars in star formation regions. Thus it is difficult to obtain a census of

their relative numbers. However, compared to field stars, NTTs are relatively strong (but variable) X-Ray sources and can be identified in X-Ray surveys. In the Taurus region such observations suggest that the population of Class III sources is at least comparable in size to that of Class II sources. Finally I note that most, but certainly not all, Weak-lined T Tauri stars (WTTS) are Class III sources. (Optical astronomers classify PMS stars with $H\alpha$ equivalent widths less than 10 Angstroms as WTTS and PMS stars with $H\alpha$ equivalent widths greater than 10 Angstroms as CTTS. Although all CTTS probably have infrared excesses, an equivalent width of 10 Angstroms is a sufficient but not necessary condition for infrared excess and some WTTS exhibit IR excess and probably have circumstellar disks)

Although most known YSOs can be classified into the three classes described above, there exist a small but significant number of objects that do not fit in to the classification scheme, at least as outlined above. These sources themselves fall into three phenomenological groups. The first, and perhaps most significant, are the *Class 0 Sources*. These objects appear to be considerably more extinguished and embedded than Class I sources. Their energy distributions peak at submillimeter wavelengths and most are not detected at wavelengths shortward of 300 μm . Their energy distributions have widths similar to single temperature black body functions, and unlike Class I sources they can be placed on the HR diagram. However, they are characterized by extremely low temperatures, 20-30 K! All are associated with energetic, very highly collimated bipolar molecular outflows. In addition, observations of YSOs in the Ophiuchi dark cloud indicate that Class 0 sources emit significantly more submillimeter radiation than do Class I objects.⁸⁰ In particular, the circumstellar mass traced by submillimeter measurements within 1000 AU of a Class I source is usually found to amount to a fraction of a stellar mass, while for a Class 0 source this mass can be comparable to that of the central star. Based on these considerations Andre, Ward-Thompson and Barsony⁸² have suggested that these sources constitute a fourth distinct class of YSO. Class 0 sources are difficult to detect and only 6 members of this group were known at the time of this writing. Consequently, it is difficult to ascertain the size of the Class 0 population in star forming regions and the significance of their role in early stellar evolution. These objects are most likely protostars in a very early stage of evolution.⁸¹ However, whether these objects are precursors of Class I sources or represent a separate branch of protostellar evolution is not yet clear.⁴¹ (It is interesting to note in this context that of the three objects possessing the best kinematic evidence of infall, two, B335 and IRAS 1629, are Class 0 sources).

A second group of objects which merit additional consideration are the so called *Flat-Spectrum Sources*. These objects have SEDs which are intermediate between Class I and Class II sources. They are characterized by a flat spectral index, i.e., $\alpha \approx 0$. In addition, they happen to be visible stars with extreme T Tauri characteristics. Indeed, the most well known member of this group is T Tauri itself. Because these objects are optically visible stars their SEDs were initially modeled as those of Class II sources possessing disks with flat temperature gradients (i.e., $n = 0.5$)⁶⁶. But

these models raised numerous difficulties and it is now apparent that these SEDs are better explained by models of infalling circumstellar envelopes with relatively large evacuated polar cavities or holes.⁸³ As such these sources are essentially Class I sources or protostars in which the accreting stellar core can be directly observed at optical wavelengths. In this context it is interesting to note that the optical spectra of these sources exhibit little in the way of photospheric absorption line features. The lack of such features is believed to be due to "veiling" by excess continuum emission generated by accretion shocks as material falls onto the stellar surface. The flat-spectrum sources appear to represent objects in transition between Class I and Class II. In fact, they may be regarded as "optical protostars".

Finally, there is a third group of sources whose SEDs exhibit complicated structure and cannot, for example, be usefully characterized by a single spectral index. These sources often have double humped spectral shapes with one peak in the optical-near infrared portion of the spectrum and another at far-infrared wavelengths. The optical and near-infrared peak or hump usually can be classified as either a Class II or Class III shape and therefore consists of mostly stellar light. The emission observed at far-infrared wavelengths may appear as a distinct peak in the SED or as an excess above an otherwise normal Class II or Class III SED. The far-infrared emission likely arises in a shell of gas and dust which surrounds a large evacuated cavity around the star. These objects are also likely transition objects similar to but perhaps in a later stage of development or viewed from a different angle than the flat-spectrum sources.

An Empirical Evolutionary Sequence: Although the SED classes (I-III) discussed above correspond to three distinct physical classes of YSOs, the variation in the shapes of the energy distributions from Class I to III is quasi continuous and for some purposes can be usefully parameterized by an SED spectral index²⁸ or a "bolometric" temperature.⁷⁹ This variation in SED shape represents a variation in the amount and distribution of luminous circumstellar material around an embedded YSO. It is natural therefore to hypothesize that the empirical sequence of spectral shapes is a sequence of the gradual dissipation of gas and dust envelopes around newly formed stars and is therefore an evolutionary sequence.²⁸ Adams, Lada and Shu⁶³ were able to theoretically model this empirical sequence as a more or less continuous sequence of early stellar evolution from protostar to young main sequence star using the self-consistent physical theory of rotating collapsing isothermal spheres as the initial condition. In this theoretical picture Class I (and Class 0) sources are the youngest and least evolved objects, indeed, true protostars, objects undergoing accretion and assembling the bulk of the mass they will ultimately contain when they arrive on the main sequence. They consist of a central embryonic (hydrostatic) stellar core surrounded by a circumstellar disk and are steadily gaining mass from accretion and infall of surrounding matter. Class III sources are the most evolved objects. For these objects the vast majority of the original star forming material has been either all incorporated into the star or removed from its vicinity. The vast majority of low mass stars probably pass through these stages during their formation. However, the fact that some Class III sources (NTTS) have similar ages as Class II sources (CTTS),

suggests that the duration of the various phases may be different for different stars, even those of similar mass.

To evolve from Class I(0)-II requires the removal or dissipation of the circumstellar material in the protostellar infalling envelope. To evolve from Class II to Class III requires clearing of the circumstellar disk. In principle, the clearing of circumstellar gas and dust could be accomplished by accreting all the surrounding material onto the star itself. However, this possibility conflicts with the observation that star formation occurs with considerable inefficiency: the cores from which stars form contain much more mass than the stars themselves, and most of the surrounding material cannot end up inside the star. This suggests that at some point very early on in the evolution of a young stellar object the cloudy material from which it grows must be physically removed by some active agent. This agent is most likely an energetic bipolar outflow which is ignited early in the protostellar stage of evolution.

5. Bipolar Molecular Outflows and Energetic Mass Ejection

In the late 1970s and early 1980s millimeter-wavelength observations of the molecular gas surrounding YSOs led to the discovery of an unanticipated phenomenon of fundamental importance for understanding star formation. In addition to their global supersonic velocity fields, molecular clouds were found to contain localized regions (0.1-3 parsecs in size) characterized by hypersonic bulk motion. In these regions the observed widths of molecular emission lines often range between 10-100 km s⁻¹. Neither gravity nor magnetic fields can confine these highly supersonic and super-Alfvénic flows to the localized regions where they occur; they must represent unbound and expanding flows of *cold* molecular gas within the GMCs.^{88,89} The regions containing the hypersonic outflows almost always coincide with, if not center on, the position of an embedded YSO, usually a Class I source. Well over 150 molecular outflows are now known,⁹³ most within a kiloparsec of the sun. Their properties have been extensively reviewed in the literature.^{90,91,92,93} Briefly, such outflows involve substantial amounts of mass, anywhere between 0.1 and 100 M_⊙. That the masses of outflows are comparable to and usually exceed the mass of the driving star indicates that the outflowing molecular gas consists of swept-up ambient cloud material rather than original ejecta from the driving source. More significantly, the flows have enormous kinetic energies, ranging between 10⁴³ and 10⁴⁷ ergs. Combining measurements of the physical dimensions and velocity fields of the outflows enables estimates of the dynamical timescales of the outflowing gas. The dynamical timescales of the flows are typically found to lie between 10³ and 10⁵ years, making their local formation rate roughly comparable to the birthrate for stars of a solar mass or greater.

Knowledge of the masses, kinetic energies and dynamical timescales of outflowing material enables determination of the mechanical luminosity and the force or thrust (i.e., the rate of momentum injection) required to drive the outflows. Both these quantities scale with the radiant luminosity of the driving stellar source.^{89,90,95} These relationships are illustrated in Figure 16 taken from the recent compilation of Cabrit and Bertout.⁹⁵ These data can be fit to produce the following two "laws":

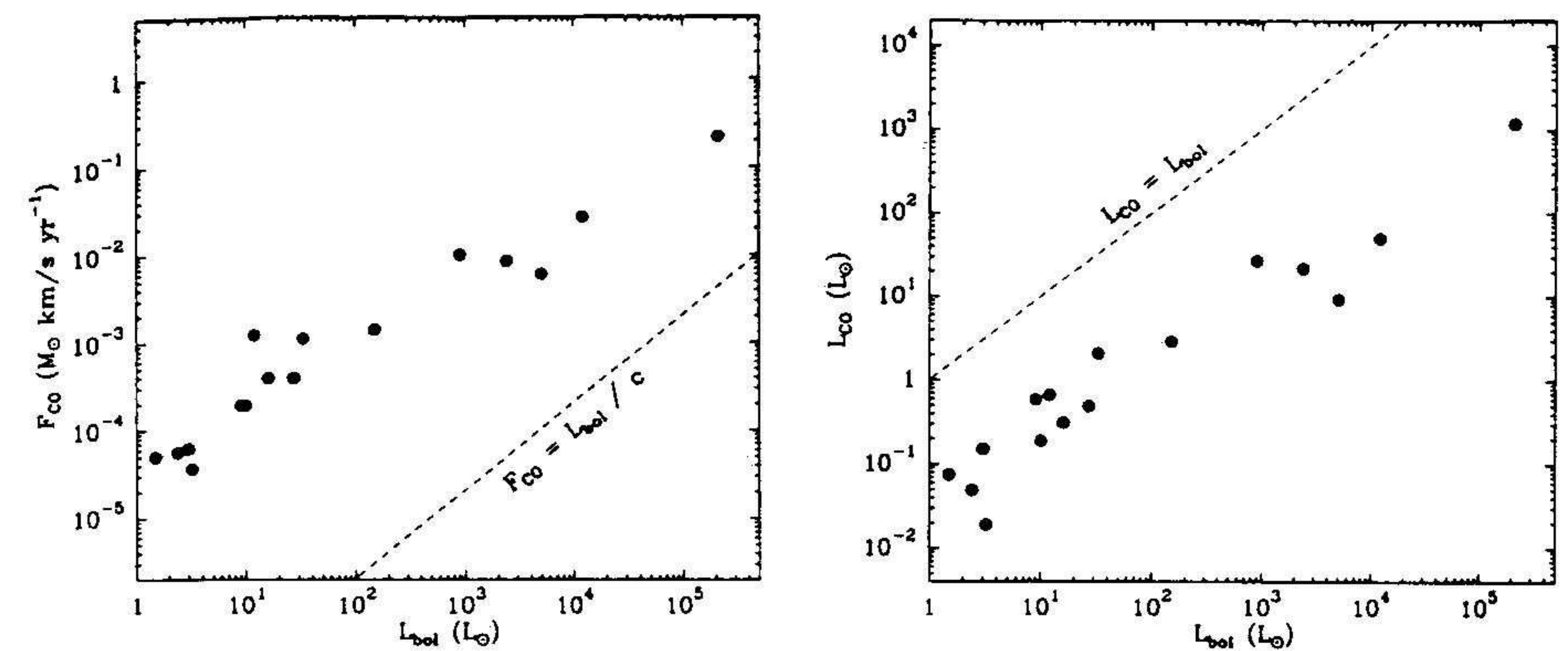


Figure 16: (Left) The outflow momentum injection rate (Force or Thrust) plotted against the bolometric luminosity of the central source. The corresponding relation for a (single scattering) radiation pressure driven wind is also shown. (Right) The outflow mechanical luminosity plotted against the bolometric luminosity of the central source. (From Cabrit and Bertout^{95,96}).

$$F_{CO}c/L_{bol} \sim 2000(L_{bol})^{-0.3} \quad \text{Force Law.}$$

and

$$L_{CO}/L_{bol} \sim 0.04(L_{bol})^{-0.2} \quad \text{Luminosity Law.}$$

(Here the luminosity is measured in units of L_⊙ and the Force in units of M_⊙km s⁻¹yr⁻¹ and c is the speed of light).

These relations provide fundamental information and constraints for understanding molecular outflows. For example, the observed relation between the force required to drive the flow (F_{CO}) and the source luminosity (L_{bol}) clearly rules out radiation pressure as a driving mechanism for molecular outflows. The relation between the flow mechanical luminosity and the radiant luminosity of the driving source indicates that a very energetic and efficient engine is required to drive the flows since L_{CO} ≈ 1-10% L_{bol}. The only reasonable reservoir of energy that can be tapped to meet such requirements is that of gravitational potential energy. Therefore, the driving engine for molecular outflows must originate near the heart of the protostar, very close to the surface of the central stellar object in the deepest part of the gravitational potential well. Bipolar molecular outflows are individually energetic enough to disrupt cloud cores and collectively powerful enough to have a significant impact on the dynamics

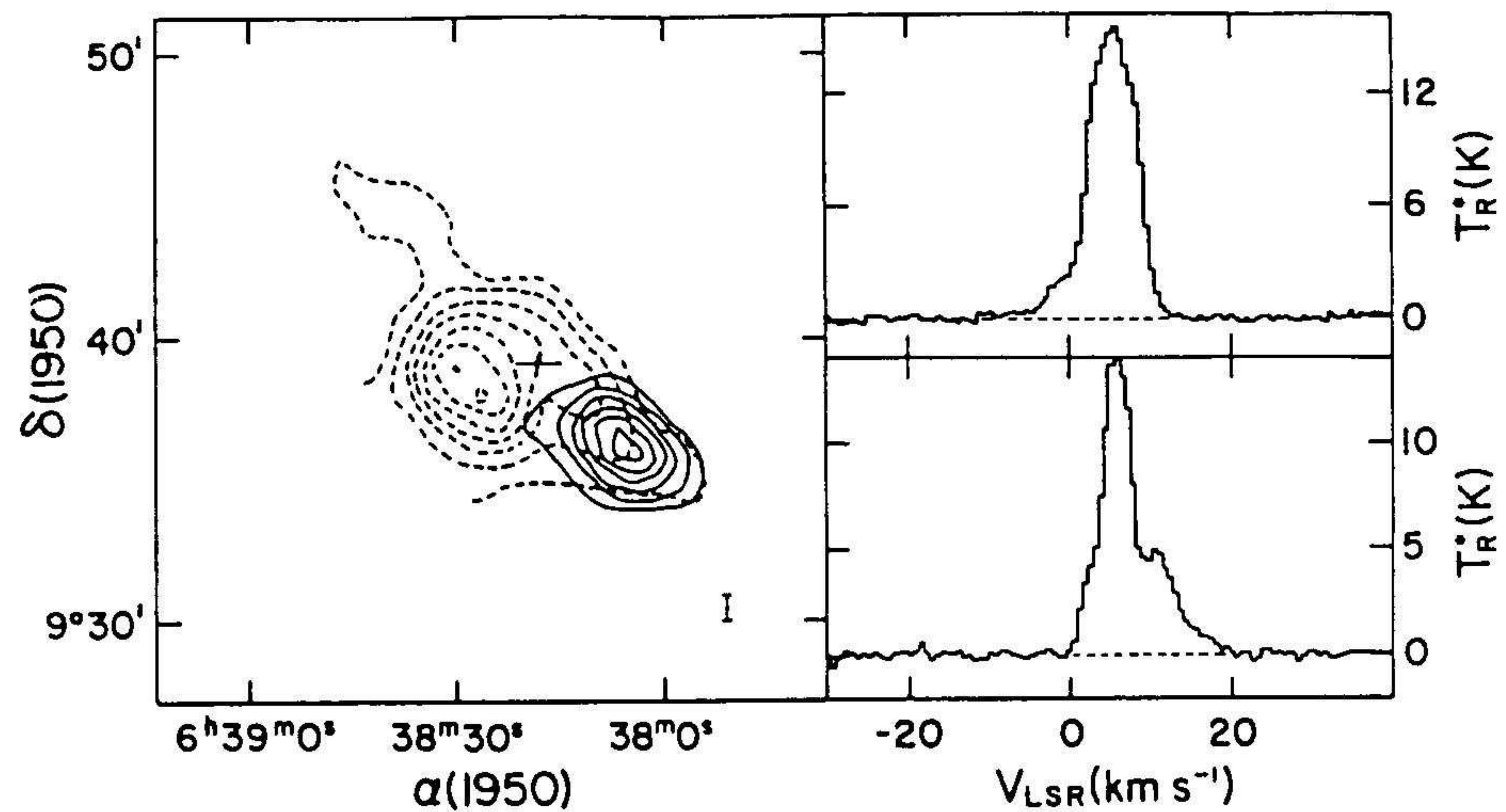


Figure 17: Map of a bipolar outflow source in the Mon OB1 (NGC 2264) molecular cloud along with representative ^{12}CO spectra observed toward each of the bipolar lobes. Dashed contours map the blue-shifted lobe and solid contours the red-shifted lobe. The position of a luminous Class I IRAS source is marked by a cross. (From Margulis, Lada and Snell⁹⁴).

and structure of an entire GMC.⁹⁴ In fact, the molecular outflows generated by a population of embedded YSOs may be able to generate the turbulent pressure that keeps GMCs from global collapse, thereby solving one of the outstanding problems of cloud dynamics.

Perhaps the most intriguing property of the molecular outflows is their tendency to appear spatially bipolar.^{88,89,90} In other words, they consist of two spatially separate lobes of emission, with one lobe containing predominantly blue-shifted gas and the other predominantly red-shifted gas. Furthermore, the two separating lobes often lie on more or less diametrically opposed sides of the embedded driving source. Figure 17 shows an example of the CO line profiles and the spatial morphology of red- and blue-shifted high velocity emission in a typical outflow source. Although most cold molecular outflows are bipolar, they are typically not very well collimated.⁹⁰ Yet outflows do exhibit a relatively wide range of spatial shapes which have been successfully explained by models with intrinsically bipolar geometries but whose inclination to the line-of-sight, opening angle and velocity field vary^{96,97,99} as illustrated in Figure 18.

Roughly 5-10% of known outflows are, however, very collimated and jet-like with

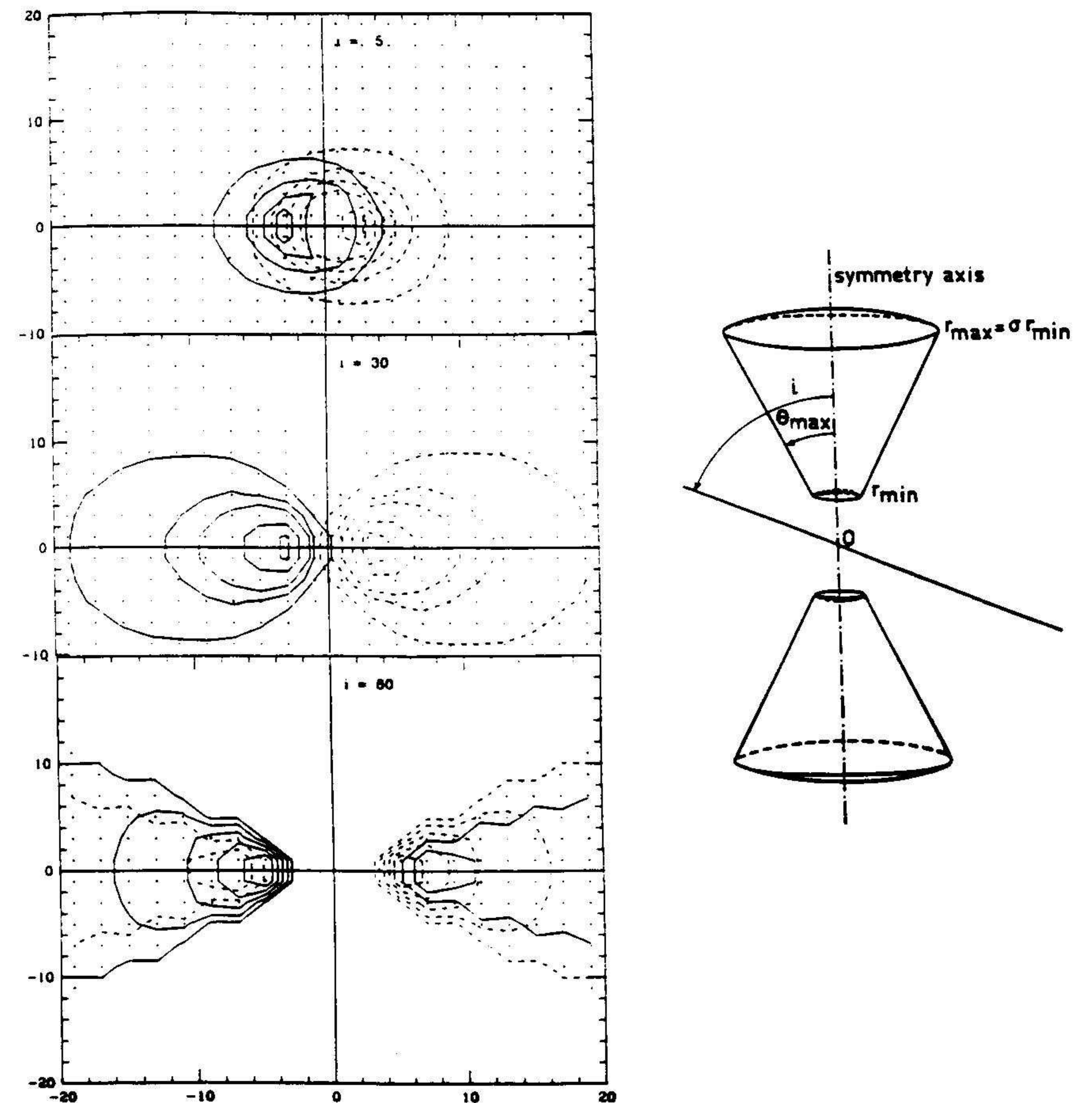


Figure 18: Model maps of a bipolar outflow with conical geometry calculated by Cabrit and Bertout for a flow with an opening angle of 30° and observed at three different angles (5° , 30° and 80°) to the line-of-sight.

aspect ratios (ratios of major to minor axes) ranging from 3 - 10. Highly collimated flows tend to be the best studied outflows and they offer additional constraints for testing theoretical models. These sources possess a number of interesting structural characteristics which can be summarized as follows:

- 1-Outflowing gas often spans a wide range of (radial) velocity (0-20 km s⁻¹ or more).
- 2-The vast majority of outflowing gas is found in the lower velocity ranges (0-10 km s⁻¹) with very little gas at the highest velocities. Indeed, the distribution of mass in the outflow appears decrease with outflow velocity in a power-law fashion.⁹⁸ Thus there appears to be no characteristic scale to the velocity field.
- 3-The lower velocity outflow gas is spatially distributed over a much larger area than the highest velocity outflow gas which is typically confined very close to the major axis of the flow "interior" to and more highly collimated than the lower velocity gas.
- 4-The highest velocity gas is often found at the ends of the outflow, down stream from the driving source. There appear to be systematic (line-of-sight) velocity gradients along the lengths of many well collimated flows. These gradients have the form of a "Hubble-like" linear progression of outflow velocity with distance from the driving source (i.e., $v \propto r$).⁹⁹
- 5-The velocity vectors of the outflowing gas appear to be largely parallel to the flow major axis with little evidence for expansion motions orthogonal to the flow major axis.⁹⁹

There is as yet no consensus concerning the physical origin of such outflows and how they are driven and collimated. Because molecular outflows consist of swept up ambient material moving primarily along the flow major axis, they are probably driven in a momentum conserving fashion by an underlying *primary* flow which itself is driven in some manner by the YSO at the heart of the system. Two classes of models have been proposed for the primary flows. In the first type, the primary flow is presumed to be an angle dependent (bipolar) wind which is driven from the star or its surrounding disk.¹⁰⁰ This wind sweeps up ambient gas in a momentum driven fashion and is probably initially collimated by either the disk or a bipolar stellar magnetic field. This type of model can successfully account for all the outflow properties listed above, except # 2, that is, such a model does not easily predict the observed line-shapes and the distribution of outflow mass with velocity. Moreover, existing models do not venture to explain either how this wind originates or how it is initially collimated. In the second type of model the primary flow is assumed to be a very fast, highly collimated, jet which entrains ambient material as it propagates into the cloud.^{98,101,102} Unfortunately it is not clear how this entrainment takes place and consequently whether or not such a jet driving model can account for any of the above outflow properties. Such models also predict more highly collimated flows than those actually observed. In addition, as with the stellar wind models, the underlying jets are assumed as initial conditions and their origin is not explained.

The primary motivation for jet driven winds results from optical observations which have revealed the presence of jets of ionized gas that appear to emanate from

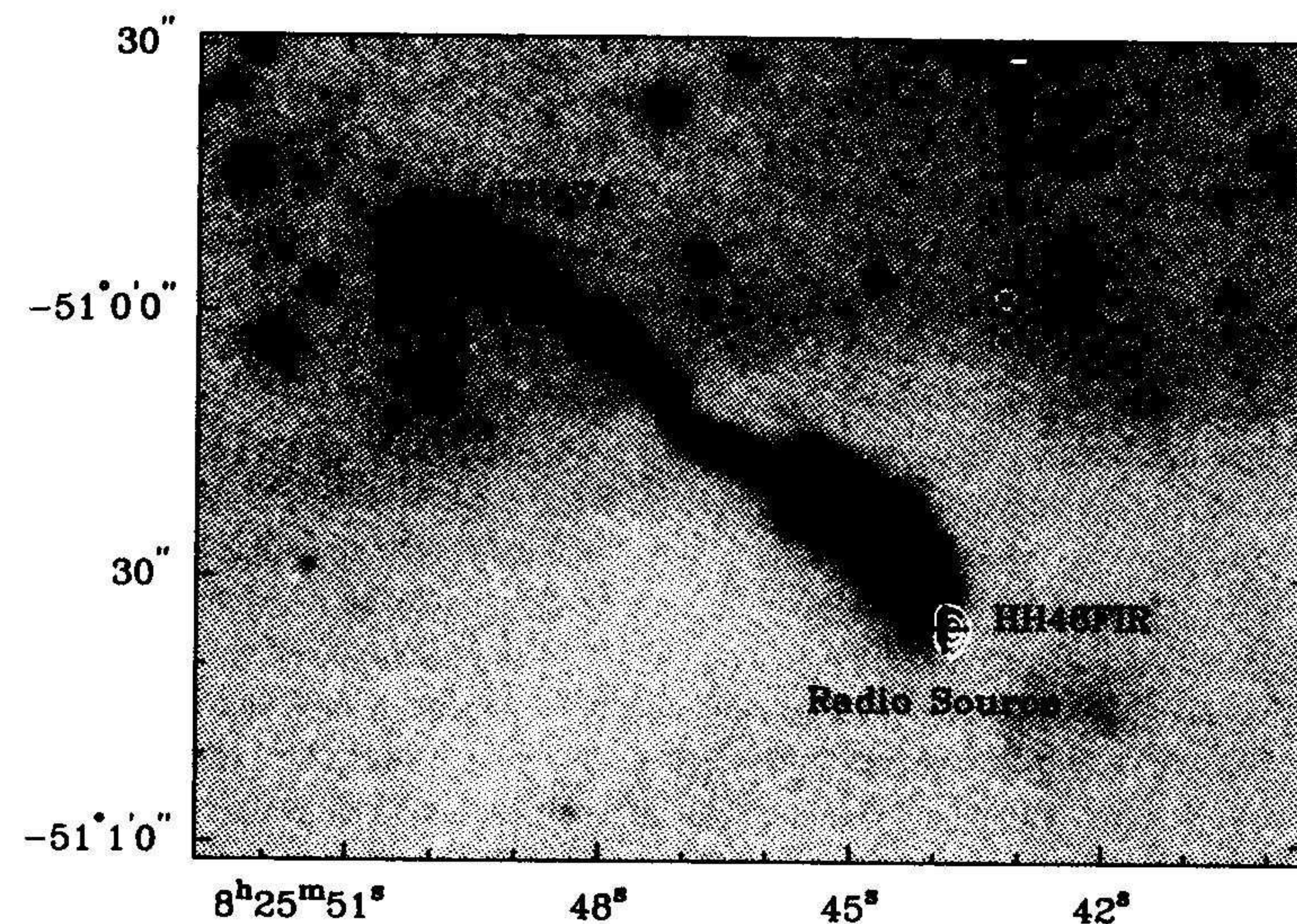


Figure 19: The optical jet associated with an embedded infrared source in a Bok globule in the Gum Nebula. This CCD image of the [SII] forbidden-line emission also shows contours of centimeter-wave radio continuum emission which coincide with the infrared source (+) driving the jet. Taken from Curiel and Wilner¹¹⁸.

very close to the surface of numerous low-mass YSOs^{103,104} (see Figure 19).¹¹⁸ These optical jets possess considerably more collimation and much higher velocity (100-400 km s⁻¹) than the larger scale bipolar molecular flows associated with low-mass YSOs. Since these jets may be energetic enough to drive molecular outflows it seems natural to try to physically link these two phenomena. However, there is also ample evidence for the presence of stellar (or disk) winds from around YSOs. It has long been known that CTTS (Class II sources) can generate powerful stellar winds.¹⁰⁵ However, to have sufficient strength to drive the molecular outflows associated with Class I sources (e.g., L1551), such stellar winds must be characterized by an appreciable mass-loss rate (e.g., 10^{-6} - 10^{-5} M_⊙yr⁻¹, at least 1-2 orders of magnitude larger than the most powerful T Tauri star winds).¹⁰⁶ Ionized stellar winds have been found around numerous Class I YSOs from both infrared spectral line and centimeter-wave radio continuum observations.¹⁰⁷ (see Figure 19) However, close examination of these ionized winds has shown that they do not contain enough momentum to drive the observed molecular outflows. The conjecture then naturally arises that a more massive and harder-to-detect neutral wind must coexist with the ionized wind.⁸⁹ In particular, models of the hydrogen recombination lines observed in the stellar winds around YSOs strongly suggest that the stellar winds have relatively low fractional ionizations.¹⁰⁶ Indeed, extremely high velocity (EHV) neutral atomic hydrogen¹⁰⁸ and CO¹⁰⁹ emission

has been observed toward a number of outflow sources. At the present time there is no unified model that can sufficiently account for the jet/wind phenomena. Whether a fast neutral stellar (or disk) wind or a fast jet is the driving source for the bipolar molecular outflows is an open question.

Another uncertain aspect of the nature of the primary flow is whether or not it is steady over the lifetime ($\approx 10^5$ yrs.)¹¹⁷ of the bipolar outflow phase. There is a growing body of evidence indicating that episodic mass ejection may be an important aspect of the pre-main sequence evolution of low mass stars.^{110,111,112} There is a subset of pre-main sequence stars (*FU Ori objects*), originally identified by Herbig,¹¹⁰ which are known to undergo intense outbursts of light. These outbursts, which can increase the luminosity of the star by a factor of 100 in a few years, are most likely due to dramatic, apparently episodic, increases in disk accretion onto the star.¹¹² During the outburst these objects eject material with very high energy and with mass loss rates ($10^{-5} M_{\odot}\text{yr}^{-1}$)¹¹² comparable to those inferred for bipolar outflows. Although originally identified optically, more than half of these objects are characterized by SEDs with Class I signatures while the rest are Class II (including FU Ori itself). Many are also found to drive molecular outflows¹¹³ (the most notable example being L1551). So it is likely that FU Ori objects are very young, some even appear to be in a late protostellar stage of evolution. It is possible that FU Ori outbursts occur throughout protostellar evolution. However, if the accretion rate ($10^{-4} M_{\odot}\text{yr}^{-1}$) which characterizes FU Ori applies to typical protostellar outbursts, we expect that as many as 5-10% of Class I sources could be in outburst at any one epoch of history (since the lifetime of a Class I source is roughly 10^5 yrs and the mass of its central star is roughly 0.5 to $1.0 M_{\odot}$). Future studies of Class I sources should be able, therefore, to assess the importance of this phenomenon for the evolution of protostars and outflows.

From the considerations discussed above it is clear that bipolar molecular outflows play central role in the formation and early evolution of stars. They are most likely the physical agent that disperses natal circumstellar gas and dust from around a protostellar object and thus drives the evolution of a newly forming star from the Class I (or 0) stage to the Class II stage. Thus bipolar outflows may have a significant influence on determining the final mass of a forming star and on the development of the stellar initial mass function. It is not yet clear at what point in the evolution of a Class I source the outflow is ignited. The statistics of Class I sources and outflows suggest that a Class I object spends a significant fraction of its lifetime as an outflow source.⁹⁰ This raises an interesting paradox.¹¹⁴ If Class I or Class 0 sources are true protostars shouldn't their evolution be characterized by the infall of surrounding material rather than outflow? How can a young star simultaneously undergo both inflow and outflow? How can a star form by losing mass? The answer to this question may be the key to understanding the basic physics of the star formation process.

The most likely source of the enormous energies which characterize gas in molecular outflows is the release of gravitational potential energy by material falling onto the surface of an embryonic star from either an infalling circumstellar envelope or from a circumstellar accretion disk. Exactly how this energy source is tapped to drive an intense stellar wind is not clear. Magnetic fields and angular momentum may play

critical roles in enabling the transfer of energy from infalling to outflowing gas. To visualize how this might work, consider a rotating infalling protostellar envelope. Because of the conservation of angular momentum the trajectories of infalling material become curved as they near the growing stellar object at the center of the potential well. As a result, most of the infalling gas misses the star and falls into the equatorial plane forming an extended disk. Consequently for a rotating protostar most of the mass that ends up on the star must be accreted from the surrounding disk. In order for material to flow through the disk and onto the protostar, the material must lose both energy and angular momentum. If the mass of the disk is not much larger than that of the central object, the material in the disk should rotate differentially in Keplerian fashion. Gas falling through such a disk will reach the surface of the central star with an orbital velocity and specific angular momentum which is relatively high compared to that in the star. If this material is added to the star it will spin up the star. The star will quickly reach break up equatorial velocities at which point material can no longer be added to it. A centrifugal barrier prevents the further growth of the protostar. Thus the process of star formation can only proceed if the incoming gas somehow can lose additional angular momentum in the process of accreting onto the star or if the star can somehow spin down while accretion is taking place.

Angular momentum can be carried away from a star by a stellar wind. *Consequently, a protostar may be able to gain mass only if it simultaneously loses mass.* To allow star formation to continue the rate of mass loss from the wind should be a fraction of the mass accretion rate i.e.,

$$\dot{M}_{wind} = f \dot{M}_{infall}$$

where the fraction f is determined by the physics of the wind generating mechanism. The ideal protostellar wind is one that carries away little mass but lots of angular momentum. A number of recent investigations have shown that centrifugally-driven hydromagnetic winds are potentially capable of doing the job.¹¹⁵ Such winds could be driven from either magnetized circumstellar disks¹¹⁵ or from the surfaces of central protostars¹¹⁶. Thus the natural consequence of star formation in rotating, magnetic cloud cores may be the formation of protostar-disk systems which generate powerful outflows and in doing so resolve the paradox of the protostar which gains mass by losing mass. An additional consequence of such "accretion driven" outflow is that as a protostar evolves, its outflow disrupts the surrounding core ultimately limiting the mass which can fall onto the central star. As the protostellar envelope disperses, the reservoir of infalling material available to drive disk accretion and mass outflow also diminishes and the YSO evolves to progressively less active states (i.e., Class I-II-III), consistent with observations and the evolutionary spectral sequence described earlier.

6. Acknowledgements

I am grateful to the Chinese Academy of Sciences, and especially the astronomers and students in Shanghai, Nanjing and Beijing for providing a stimulating atmosphere and gracious hospitality during the 7th Guo Shoujing Summer School on Astrophysics.

This paper is based on a series of lectures presented at that school. I also thank Chi Yuan for inviting me to participate in this undertaking and for his masterful organization of the enterprise.

7. References

1. M. S. Roberts, *P.A.S.P.* **69** (1957) 59.
2. A. Blaauw, *A.R.A.A.* **2** (1964) 213.
3. C. J. Lada and E. A. Lada in *The Formation and Evolution of Star Clusters*, ed. K. Janes (ASP, San Francisco, 1991), p. 3.
4. B. J. Bok, *Harvard Circ. No.* **384**.
5. A. Blaauw in *The Physics of Star Formation and Early Stellar Evolution*, eds. C.J. Lada and N.D. Kylafis, (Kluwer Academic Publishers: Dordrecht, 1991), p. 125.
6. B. G. Elmegreen and C. J. Lada, *Astron. J.*, **81** (1976), 1089.
7. B. G. Elmegreen and C. J. Lada, *Astrophys. J.*, **214** (1977), 725.
8. H. A. Abt and S. Levy, *Astrophys. J. Suppl. Ser.*, **30** (1976), 273.
9. A. Duquennoy and M. Mayor *Astron. Astrophys.*, **248** (1991), 485.
10. D. Fischer and G. Marcy *Astrophys. J.*, **396** (1992), 178.
11. T. S. van Albada in *Birth and Evolution of Massive Stars and Stellar Groups*, eds. H. van Woerden and W. Boland, (Reidel: Dordrecht, 1985), p. 89.
12. D. Mihalas and J. Binney *Galactic Astronomy*, (Freeman: San Francisco), p. 217.
13. E. Salpeter, *Astrophys. J.*, **121** (1955) 161.
14. M. Schwarzschild, *Structure and Evolution of Stars*, (Princeton University Press: Princeton).
15. C. W. Allen, *Astrophysical Quantities*, (Athlone Press: London).
16. J. Scalo in *Fundamentals of Cosmic Physics*, **11**, 1.
17. P. Kroupa, C. Tout and G. Gilmore, *Monthly Notices Roy. Astron. Soc.*, **244** (1990) 76.
18. M. F. Walker *Astrophys. J. Suppl. Ser.*, **2** (1956) 365.
19. F. Palla and S. W. Stahler, *Astrophys. J.*, **418** (1993) 414.
20. S. W. Stahler, *Astrophys. J.*, **274** (1983) 822.
21. C. Hayashi, *Ann. Rev. Astron. Astrophys.*, **4** (1966) 171.
22. L. G. Henyey, R. LeLevier and R. D. Levee *Publ. Astron. Soc. Pacific*, **67** (1955) 154.
23. L. Blitz, in *Giant Molecular Clouds in the Galaxy*, eds. P. Solomon and M. Edmunds, (Pergamon, Oxford, 1980) p. 1.
24. P. Goldreich and J. Kwan, *Astrophys. J.*, **89** (1974) 441.
25. B. Zuckerman and N. Evans, *Astrophys. J. Letters*, **187** (1974) 67.
26. R. Duerr, K. Imhoff and C. J. Lada *Astrophys. J.*, **261** (1982) 135.
27. A. Whitworth, *Monthly Notices Roy. Astron. Soc.*, **186** (1979) 59.
28. C. J. Lada in *I.A.U. Symposium No. 115: Star Forming Regions*, eds. M. Peimbert and J. Jugaku, (Dordrecht, Reidel, 1987), p. 1.
29. C. Heiles. A. A. Goodman, C. F. McKee, E. Zweibel in *Protostars and Planets III*, eds. G. Levy and J. Lunine, (University of Arizona Press, Tucson, 1993) p. 279.
30. T. Mouschovias *Astrophys. J.*, **207** (1976) 141.
31. T. Mouschovias in *The Physics of Star Formation and Early Stellar Evolution*, eds. C.J. Lada and N.D. Kylafis, (Kluwer Academic Publishers: Dordrecht, 1991), p. 61.
32. L. Blitz, in *The Physics of Star Formation and Early Stellar Evolution*, eds. C.J. Lada and N.D. Kylafis, (Kluwer Academic Publishers: Dordrecht, 1991), p. 3.
33. J. Scalo, in *Protostars and Planets II*, eds. D. Black and M. S. Matthews, (University of Arizona Press: Tucson), p. 201.
34. J. Scalo, in *Physical Processes in Fragmentation and Star Formation*, eds. R. Capuzzo-Dolcetta, C. Chiosi and A. Di Fazio (Dordrecht, Kluwer 1990) p. 151.
35. R. L. Dickman, M. A. Horvath, M. Margulis *Astrophys. J.*, **365** (1990) 586.
36. E. A. Lada, J. Bally and A. Stark, *Astrophys. J.*, **368** (1991) 432.
37. K. Tatematsu *et al.*, *Astrophys. J.*, **404** (1993) 643.
38. D. Clemens and R. Barvanis, *Astrophys. J. Suppl. Ser.*, **68** (1988) 257.
39. P. Benson and P. Myers *Astrophys. J. Suppl. Ser.*, **71** (1989) 89.
40. R. Loren, *Astrophys. J.*, **338** (1989) 902.
41. C. J. Lada in *The Physics of Star Formation and Early Stellar Evolution*, eds. C.J. Lada and N.D. Kylafis, (Kluwer Academic Publishers: Dordrecht, 1991), p. 329.
42. R. B. Larson, *Monthly Notices Roy. Astron. Soc.*, **194** (1981) 271.
43. P. C. Myers and A. Goodman, *Astrophys. J.*, **329** (1988) 392.
44. P. C. Myers in *Protostars and Planets II*, eds. D. Black and M. S. Matthews, (University of Arizona Press: Tucson), p. 81.
45. G. A. Fuller and P. C. Myers, *Astrophys. J.*, **384** (1992) 583.
46. E. A. Lada, D. L. DePoy, N. J. Evans, and I. Gatley, *Astrophys. J.*, **371** (1991) 171.
47. E. A. Lada, *Astrophys. J. Letters*, **393** 25.
48. R. D. Mathieu, in *I.A.U. Symposium No. 115: Star Forming Regions*, eds. M. Peimbert and J. Jugaku, (Dordrecht, Reidel, 1987), p. 61.
49. P. G. Murden and M. V. Penston, *Monthly Notices Roy. Astron. Soc.*, **181** (1977) 657.
50. H. Zinnecker, M. McCaughrean and B. Wilking, in *Protostars and Planets III*, eds. G. Levy and J. Lunine, (University of Arizona Press, Tucson, 1993) p. 429.
51. S. Wiramihardja *et al.* *Publ. Astron. Soc. Japan*, **43** (1991) 27.
52. K. M. Strom, S. E. Strom and M. Merrill *Astrophys. J.*, **412** (1993) 233.
53. E. A. Lada, K. M. Strom, P. C. Myers, in *Protostars and Planets III*, eds. G. Levy and J. Lunine, (University of Arizona Press, Tucson, 1993) p. 245.

54. M. Gomez, L. Hartmann, S. Kenyon, and R. Hewett *Astron. J.*, **105** (1993) 1927.
55. H. Chen, A. Tokunaga, K. Strom, and K.-W. Hodapp *Astrophys. J.*, **407** (1993) 639.
56. C. J. Lada, M. Margulis and D. Dearborn, *Astrophys. J.*, **285** (1984) 141.
57. A. Gehz, Unpublished PhD Dissertation, Cal Tech (1993).
58. Ch. Leinert, *et al. Astron. Astrophys.*, **278**, (1993) 129.
59. C. Prosser, *et al. Astrophys. J.*, **421** (1994) 517.
60. A. Fletcher and S. Stahler *Astrophys. J.*, (1994: in press).
61. E. A. Lada and C. J. Lada *Astrophys. J.*, (1994: in press).
62. C. J. Lada, E. T. Young, and T. Greene, *Astrophys. J.*, **408** (1993) 471.
63. F. C. Adams, C. J. Lada and F. Shu, *Astrophys. J.*, **312** (1987) 788.
64. C. J. Lada and B. A. Wilking, *Astrophys. J.*, **287** (1984) 610.
65. S. M. Rucinski, *Astron. J.*, **90** (1985) 2321.
66. F. C. Adams, C. J. Lada and F. Shu, *Astrophys. J.*, **326** (1988) 825.
67. P. C. Myers *et al.*, *Astrophys. J.*, **319** (1987) 340.
68. B. A. Wilking, C. J. Lada and E. T. Young, *Astrophys. J.*, **340** (1989) 823.
69. S. J. Kenyon L. Hartmann, S. E. Strom and K. M. Strom, *Astron. J.*, **99** (1990) 869.
70. D. Lynden-Bell and J. Pringle, *Monthly Notices Roy. Astron. Soc.*, **168** (1974) 168.
71. F. C. Adams and F. Shu, *Astrophys. J.*, **308** (1986) 836.
72. M. Friedjung, *Astron. Astrophys.*, **146** (1985) 336.
73. S. Kenyon and L. Hartmann, *Astrophys. J.*, **323** (1987) 714.
74. S.V.W. Beckwith, A. I. Sargent, R. Chini, R. Gusten, *Astron. J.*, **99** (1990) 924.
75. C. Bertout and G. Basri, in *The Physics of Star Formation and Early Stellar Evolution*, eds. C.J. Lada and N.D. Kylafis, (Kluwer Academic Publishers: Dordrecht, 1991), p. 649.
76. S. Edwards, *et al.*, *Astrophys. J.*, **321** (1987) 473.
77. I. Appenzeller, I. Jankovics, and R. Ostreicher, *Astron. Astrophys.*, **141** (1984) 108.
78. F. Walter, *Publ. Astron. Soc. Pacific*, **99** (1987) 31.
79. P. C. Myers and Ladd E. F., *Astrophys. J. Letters*, **413** (1993) 47.
80. P. Andre and T. Montmerle, *Astrophys. J.*, **420** (1994) 837.
81. P. Andre, in *The Cold Universe*, eds. T. Montmerle, C.J. Lada, F. Mirabel and J. Tran Thanh Van, (Paris, 1994) in press.
82. P. Andre, D. Ward-Thompson, and M. Barsony, *Astrophys. J.*, **406** (1993) 122.
83. N. Calvet, L. Hartmann, S. Kenyon and B. Whitney, preprint (1994).
84. S. Zhou, N. J. Evans II, C. Kompe and C. M. Walmsley, *Astrophys. J.*, **404** (1993) 232.
85. C. K. Walker, C. J. Lada, P. Maloney, E. Young and B. Wilking, *Astrophys. J. Letters*, **309** (1986) 47.

86. G. Grasdalen, G. Sloan. N. Stout, S. Strom, A. Welty, *Astrophys. J.*, **339** (1989) 37.
87. M. Hayashi, N. Ohashi and S. M. Miyama, *Astrophys. J. Letters*, **418** (1993) 71.
88. R. Snell, R. Loren and R. Planbeck, *Astrophys. J. Letters*, **239** (1980) 17.
89. J. Bally and C. J. Lada, *Astrophys. J.*, **265** (1983) 824.
90. C. J. Lada, *Ann. Rev. Astron. Astrophys.*, **23** (1985) 267.
91. J. Bally and A. P. Lane in *The Physics of Star Formation and Early Stellar Evolution*, eds. C.J. Lada and N.D. Kylafis, (Kluwer Academic Publishers: Dordrecht, 1991), p. p 471.
92. R. Bachiller and J. Gomez-Gonzalez, *Astr.Ap.Rev.*, **3** (1992) 257.
93. Y. Fukui *et al.*, in *Protostars and Planets III*, eds. E. H. Levy and J. I. Lunine, (Arizona: Tucson), (1993) p. 603
94. M. Margulis, C. J. Lada and R.N. Snell, *Astrophys. J.*, **333** (1989) 316.
95. S. Cabrit and C. Bertout, *Astron. Astrophys.*, **261** (1992) 274.
96. S. Cabrit and C. Bertout, *Astrophys. J.*, **307** (1986) 313.
97. S. Cabrit and C. Bertout, *Astrophys. J.*, **348** (1990) 530.
98. C. Masson and L. Chernin, *Astrophys. J. Letters*, **414**, 230.
99. B. Meyers-Rice and C. J. Lada, *Astrophys. J.*, **368** (1991) 445.
100. F. H. Shu, S. P. Ruden, C. J. Lada and S. Lizano, *Astrophys. J. Letters*, **370** (1991) 31.
101. A. Raga, J. Canto, N. Calvet, L. Rodriguez, J. Torrelles, *Astron. Astrophys.*, **276** (1993) 539.
102. L. Chernin, C. Masson, E. A. G. Dal Pino and W. Benz, *Astrophys. J.*, (in press: 1994)
103. R. Mundt, in *Protostars and Planets II*, eds. D. Black and M. S. Matthews, (University of Arizona Press: Tucson), p. (1985) p. 414.
104. B. Reipurth in *The Physics of Star Formation and Early Stellar Evolution*, eds. C.J. Lada and N.D. Kylafis, (Kluwer Academic Publishers: Dordrecht, 1991), p. 497.
105. G. Herbig, in *Adv.Astr.Ap* **1** (1962) 47.
106. A. Natta, in *The Physics of Star Formation and Early Stellar Evolution*, eds. C.J. Lada and N.D. Kylafis, (Kluwer Academic Publishers: Dordrecht, 1991), p. 595.
107. N. Panagia, in *The Physics of Star Formation and Early Stellar Evolution*, eds. C.J. Lada and N.D. Kylafis, (Kluwer Academic Publishers: Dordrecht, 1991), p. 565.
108. S. Lizano *et al.*, *Astrophys. J. Letters*, **328** (1988) 763.
109. M. Margulis and R. Snell, *Astrophys. J.*, **343** (1989) 779.
110. G. Herbig, *Astrophys. J.*, **217** (1977) 693.
111. B. Reipurth, *Nature* **340** (1989) 42.
112. L. Hartmann, in *The Physics of Star Formation and Early Stellar Evolution*, eds. C.J. Lada and N.D. Kylafis, (Kluwer Academic Publishers: Dordrecht, 1991), p. 623.

113. N. J. Evans *et al.*, *Astrophys. J.*, **424** (1994) 793.
 114. C. J. Lada and F. H. Shu, *Science*, **1111** (1990) 1222.
 115. R. Pudritz, G. Pelletier, A. I. Gomez de Castro, in *The Physics of Star Formation and Early Stellar Evolution*, eds. C.J. Lada and N.D. Kylafis, (Kluwer Academic Publishers: Dordrecht, 1991), p. 539.
 116. F. H. Shu, S. Lizano, S. Ruden and J. Najita, *Astrophys. J. Letters*, **328** (1988) 19.
 117. N. D. Parker, R. Padman, P. Scott and R. Hills, *Monthly Notices Roy. Astron. Soc.*, **234** (1991) 442.
 118. S. Curiel and D. Wilner, in preparation (1994).

STAR-FORMING MOLECULAR CLOUDS

P. C. MYERS

*Harvard-Smithsonian Center for Astrophysics
 60 Garden Street, Cambridge MA 02138 USA*

ABSTRACT

Molecular clouds, their star-forming condensations, and their youngest associated stars are described from an observational viewpoint. Specific topics include the star-forming galaxy; molecular cloud properties; techniques for observing molecular clouds; interpreting cloud observations; "types" of molecular clouds; relationships among cloud kinetic, gravitational, and magnetic energy; star-forming cloud condensations and their properties; the youngest stars; and searches for gravitational infall.

1. Introduction

Stars are the fundamental units of astronomy, and their origin is a fundamental problem in astrophysics. The formation of one particular star, the Sun, and its planets is also of fundamental importance for our understanding of the origin and evolution of life on Earth. These questions about star formation are ancient and difficult: they have been asked throughout human history, and they remain unsolved today.

In the last 30 years tremendous progress has been made in understanding the *circumstances* of star formation. Radio and millimeter wavelength observations have revealed and elucidated the molecular clouds which harbor all young stars; the dense cores of molecular clouds, which contain the youngest stars known, and the molecular outflows which help dissipate the prestellar gas. Infrared observations have identified the youngest stars, visible only to infrared and radio telescopes, and have revealed the size, number, and luminosity of their characteristic groups. Important steps have also been made in understanding the *processes* of star formation, through models of gravitational infall, and the interaction of magnetic, hydrodynamic, and gravitational forces in star-forming clouds. "Star formation" is now one of the fastest-growing and most active fields in astrophysics.

Table 1. Some size scales for star formation.

Object	Log size scale (cm)
galactic spiral arm	22
giant molecular cloud	20
dense core	17
accretion disk	15
protostar	11

Star formation has many size scales, some of which are indicated in Table 1. The